EXPERIMENTAL MEASUREMENT OF BLOOD PRESSURE IN 3-D PRINTED HUMAN VESSELS

by

John Talamantes Jr.

A Thesis

Submitted to the Faculty of Purdue University

In Partial Fulfillment of the Requirements for the degree of

Master of Science in Mechanical Engineering

Department of Mechanical and Energy Engineering

Indianapolis, Indiana

May 2022

THE PURDUE UNIVERSITY GRADUATE SCHOOL
STATEMENT OF COMMITTEE APPROVAL

Dr. Huidan (Whitney) Yu, Chair

Department of Mechanical and Energy Engineering

Dr. Jie Chen

Department of Mechanical and Energy Engineering

Dr. Likun Zhu

Department of Mechanical and Energy Engineering

Approved by:

Dr. Jie Chen

For My Parents and Brothers

ACKNOWLEDGMENTS

Throughout my time as a master's student, several people have played a part in my success. Without them, the completion of this work would have not been possible. Therefore, I would like to thank the following people for their contributions, however big or small.

First and foremost a special thanks to my academic advisor Dr. Whitney Yu for the opportunity to be a part of her lab group. She has offered a great deal of advice, patience and motivation. I have learned much from her sharing her experience with me and will continue to draw upon those lessons in the future.

I would like to thank Dr. Jie Chen and to Dr. Likun Zhu from Mechanical Engineering for agreeing to be on my committee.

The contributions of Dr. Alan Sawchuk have been important throughout this work. I am grateful for his support and guidance.

A special thanks to Michael Golub for supporting the lab with equipment(sometimes on very short notice) and advice.

I would like to especially thank Mr. Jerry Mooney for his guidance and support. His help made an enormous difference and without it, this would not have been possible.

Much appreciation to Dr. Julia Arciero for bringing some enlightenment to the background and theory of this work.

The contributions of MURI students, Meredith Buganski and Charles Rumburger made an enormous impact. Their dedication and hard work were key in moving this experiment forward.

My lab mate, Mr. Weichen Hong has been supportive and valuable in providing insights into this research. I thank him for his easy-going nature and for his support.

Finally, the friendship and support of Michaela Gilbert and Joseph Derrick were immensely helpful throughout this master's thesis. I am thankful to them for many amusing distractions and at times, an ear to bend.

PREFACE

Measurement of patient physiological conditions, such as blood pressure, can be conducted through numerous procedures, such as a non-invasive arm-cuff to more invasive methods such as the insertion of a pressure-tipped catheter wires. Measuring more accurate and even local pressures can be useful when a patient is experiencing any number of the diseases that are associated with the Cardiovascular System. These can involve the use of catheter wires being guided slowly through the arterial tree to find a localized point where pressure must be measured. Is it possible to develop other ways in which this patient data can be obtained? Could an approach involve a non-invasive method using patient data and computed tomography scans? Would it maintain accuracy while providing useful information to medical professionals? This work seeks an approach in which this is investigated.

TABLE OF CONTENTS

LIST OF TABLES

LIST OF FIGURES

LIST OF SYMBOLS

m	Mass
v	Velocity
r	Proximal Resistance
R	Distal Resistance
C	Arterial Compliance
Q	Volumetric Flow Rate
A	Area
μ	Viscosity
t	Time
L	Length

ABBREVIATIONS

FFR	Fractional Flow Reserve
TSPG	Trans-Stenosit Pressure Gradient
RCIA	Right Common Iliac Artery
REIA	Right External Iliac Artery
RIIA	Right Internal Iliac Artery
SV	Stroke Volume
CFD	Computational Fluid Dynamics
CVD	Cardiovascular Disease

ABSTRACT

A pulsatile flow loop can be suitable for measurement of in vitro blood pressure. The pressure data collected from such a system can be used for evaluating stenosis in human arteries, a condition in which the arterial lumen size is reduced. The objective of this work is to develop an experimental system to simulate blood flow in the human arterial system. This system will measure the in vitro hemodynamics using 3-D prints of vessels extracted from patient CT images. Images are segmented and processed to produce 3-D prints of vessel geometry, which are mounted in the loop. Control of flow and pressure is made possible by the use of components such as a pulsatile heart pump, resistance, and compliance elements. Output data is evaluated by comparison with CFD and invasive measurement. The system is capable of measurement of the pressures such as proximal, Pa, and distal, Pd, pressures to evaluate in vivo conditions and to assess the severity of stenosis. This is determined by use of parameters such as fractional flow reserve (FFR=P_d/P_a) or trans-stenotic pressure gradient (TSPG=P_a-P_d). This can be done on a non-invasive, patient specific basis, to avoid the risk and high cost of invasive measurement.

In its operation, the preliminary measurement of blood pressures demonstrates agreement with the invasive measurement as well as the CFD results. These preliminary results are encouraging and can be improved upon by continuing development of the experimental system. A working pulsatile loop has been reached, an initial step taken for continued development. This loop is capable of measuring the flow and pressure from in a 3-D printed artery. Future works will include more life-like material for the artery prints, as well as cadaver vessels.

1. INTRODUCTION

The diseases of the cardiovascular system are of significant interest to health care professionals. An increasing number of studies are being conducted to better understand the characteristics of cardiovascular flows. A better understanding of these properties can allow researchers an insight into the origins of various cardiovascular diseases and the approaches by which they can be treated. These diseases are defined as any condition which affects the heart or vessels (veins and arteries). Every year cardiovascular diseases (CVD) account for 18.6 million deaths worldwide CVD is the number one cause of death worldwide [1], [2]. High blood pressure is notable in that it can be a precursor to worsening conditions. In combination with other risk factors can lead to organ damage in the kidneys or lead to hardening and narrowing and subsequent hardening of the arteries, which can lead to heart attack or stroke. These conditions are further contributed to by lifestyle choices such as poor diet and smoking. In the US, nearly half of adults (47% or 116 million) have hypertension or are taking medication to control hypertension. Hypertension is defined as a systolic blood pressure greater than 130 mmHg and a diastolic pressure greater than 80 mmHg. In 2019 over half a million deaths had hypertension as a primary or contributing factor [3]. A more focused investigation of the interaction between blood pressure and blood flow can provide more insight into the cardiovascular conditions of a patient. This can be accomplished by the study of hemodynamics.

1.1 Background in the Study of Hemodynamics

The study of flowing blood, known as hemodynamics, has a history that reaches back several hundred years. Beginning in the 1600s English physician William Harvey reasoned that blood circulates continuously. Discovery in the study of hemodynamics continued with measurement of arterial pressure by Hales in the 18th century [4], as well as the establishment of a relationship between the elastic properties of arteries and the propagation speed of the arterial pulse [5]. The function of the cardiovascular system begins as the left ventricle of the heart fills and then contracts to expel blood. The arteries expand in sync with the contraction of the heart [6]. The cardiovascular system consists of the heart and a vessel

network. Blood containing nutrients and oxygen flow through the network of vessels to transport them throughout the body [5]. Each contraction of the heart creates the pressure which pushes blood through the vascular network. This can be modeled as liquid flow through a pipe, which will make use of the Poiseuille laws of pipe flow as a basis to describe flowing blood through arteries. This is demonstrated in Fig. 1.1.

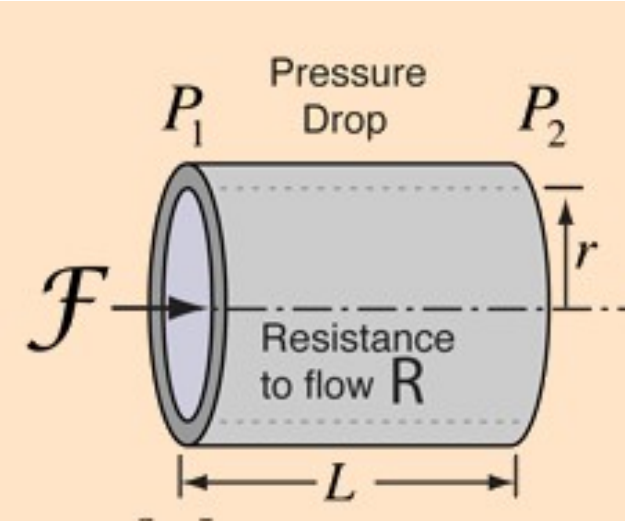

Figure 1.1. The pressure drop across the length of vessel is the basis for the Poiseuille law. This will be applied to blood flow through the vascular system of arteries. [7]

As the blood reaches organs, oxygen and nutrients are exchanged with the surrounding tissue. Simultaneously, waste products are also exchanged and transported to be expelled from the body upon returning blood to the venous system to repeat the process.

In addition to oxygen and nutrients, fatty and mineral deposits are also transported through the circulatory system. Increased blood lipoproteins accumulate in the intima layer of arteries. The plaques that form continue to grow thereby reducing the blood flow. As calcium and connective tissue proliferate within the lesion, stenosis, or narrowing of the artery is formed. A resulting uneven surface forms on the inner surface of arteries. The further formations of a clot and thrombosis lead to the obstruction of blood flow [8]. Risk factors that can hasten this process are hypertension, smoking, sedentary lifestyle, diabetes,

and poor diet. Abnormalities in flow can cause changes in the conditions in a patient, such as higher blood pressure or hypertension.

The American Heart Association (AHA) considers blood pressure to be normal when the systolic pressure is below 120 mmHg and the diastolic pressure below 80 mmHg. AHA uses a systolic of between 120 to 139 and a diastolic of between 80 to 89 as the baseline for "pre-hypertension". Thus, a BP above 140/90 mmHg is considered to be high blood pressure. Hypertension is one of the risk factors associated with the formation of atherosclerotic lesions. These lesions are prone to form near branch points or bifurcations which are areas characterized by low shear, turbulence and oscillating flows [9], [10]. Increases in the concentration of low-density lipoprotein (LDL) in the blood lead to accumulations of LDL in the intima (innermost tunica) of the vessel. The accumulated lipoprotein becomes oxidized and pathological. Sub-endothelial plaque emerges into the artery lumen, the lipoproteins begin as microscopic foci, progress to fatty streaks to enlarged plaques which become calcified. Local hemodynamics can have a significant influence on the early stages of atherosclerosis and the formation of plaques [9], [11], [12]. The plaques can continue to progress, significantly reducing the artery lumen and reducing blood flow. This process can continue further to complete occlusion of the vessel. Occlusion can lead to tissue damage and organ failure by a reduced flow of blood through the vessels, which is known as ischemia. This can occur in any portion of the body, such as the brain (cerebral ischemia), the heart (myocardial ischemia), or the legs (critical limb ischemia). This reduction in blood flow will result in parts of the body which do not receive adequate oxygen. This lack of oxygen will lead to conditions such as strokes in the case of brain ischemia or organ failure. The accumulating plaques are the condition which inspired this work and as such, they will be the main focal point.

1.2 Stenosis

The narrowing of the vessel is known as stenosis. This accumulation of plaques formed during the atherosclerosis process over time can continue up to the point of partial or complete occlusion of a vessel. Which is shown in Fig. 1.2.

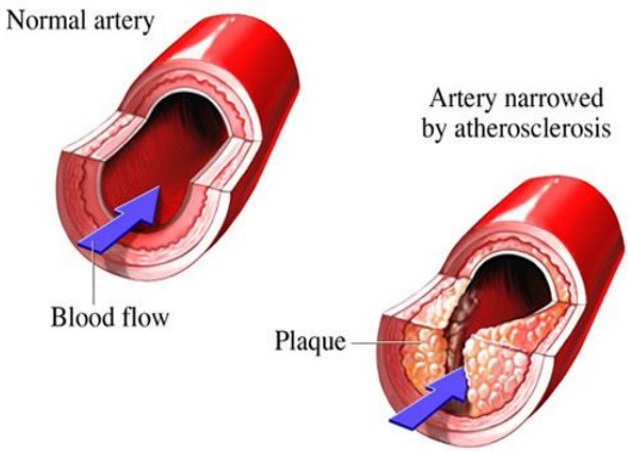

Figure 1.2. The process of Atherosclerosis can accumulate substances which reduce the artery lumen through which blood flows. IMAGE: [13]

This can most commonly occur in larger arteries in the vascular tree, such as the renal, iliac, or carotid arteries. As the plaques accumulate a reduction in cross-sectional area can increase the resistance to the flow. The increase in resistance, which results from the reduced lumen through which blood flows, has a corresponding local increase in blood pressure. This creates an increased pressure gradient across the stenosis. Some hemodynamics effects can be more local and contained in a smaller region of a vessel, as shown in Fig. 1.3. For example, the effect can be local in the form of turbulent flows and increased pressure gradient which can exist at a bend or bifurcation. Or it can be more systemic in nature such as hypertension which can affect the heart or kidneys in other parts of the body. Disruptions in flow, such as turbulence, or increased pressure can negatively affect the organ function. For example, disruptions in renal artery flow can negatively affect the function of the kidneys, and lead to renal failure. This turbulence can affect the flow of blood by reducing the flow as the pressure difference is increased [14].

This study focuses on a stenosed iliac artery. By reducing the flow through the iliac artery, the lower extremities in the leg can be adversely affected and result in symptoms such as leg pain, numbness, or necrosis of leg tissue [2]. The most extreme case can result in the loss of the leg.

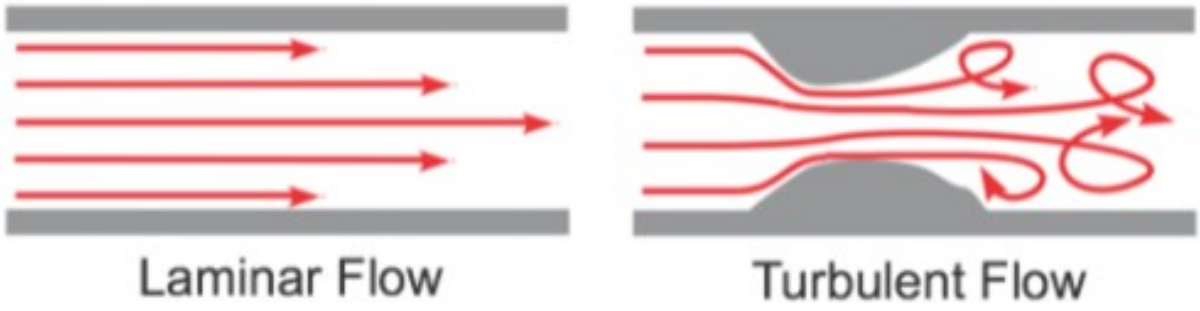

Figure 1.3. Blood flowing through a healthy artery and a stenosed artery – The flow regime shown in a healthy artery that contains Laminar Flow; the stenosed artery on the right contains turbulent flow. IMAGE: [14]

1.3 Research Motivation

The motivation for this work comes from a desire to evaluate blood pressure using a non-invasive approach. Complications in patient care that could harm the patient include infection, nerve damage, and damage to adjacent tissue [15]. Hemodynamic effects of invasive methods such as catheter wire measurement through stenosis can involve the catheter interference with flow through the artery lumen. As blood pressure is an important parameter in the evaluation of cardiovascular disease, accurate measurement is important. Possible inaccuracies can originate from catheter wires placed through the reduced lumen caused by a stenotic lesion. Irregularities in wall shear stress, flow velocity, and pressure gradient can exist with the catheter wire further reducing the artery lumen it passes through, shown in Fig. 1.4. This allows for the possibility of increases in pressure gradient, due to the increase in pressure at the proximal entrance to the throat of the stenosis. The catheter wire is on the same order of magnitude as the vessel, thus the catheter wire insertion is significant to the flow when inserted[16]. The reduction in radius through the lumen can have the added effect of increasing the local resistance, which will be a result of the increase in gradient, ΔP [17].

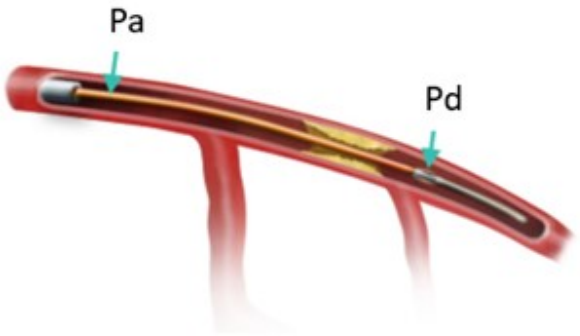

Figure 1.4. Catheter Insertion Through a Stenosed Artery - The reduced Vessel Lumen Further Occluded as the Catheter Wire is Inserted. IMAGE: [18]

The use of non-invasive methods can aid in obtaining pressure measurements while avoiding the disruptions to the flow described above. This approach can be more cost-effective, more accurate, and safer for the patient. This evaluation can take many approaches. One such method can take an image-based approach. Which will evaluate the parameters which affect blood pressure and flow. This approach makes use of medical imaging and patient data to create 3-D prints of diseased arteries for use with experimental methods to simulate in vivo conditions. By seeking to recreate the in vivo conditions, we can better evaluate the parameters present within the vascular network or a single vessel. These parameters can aid in understanding the physical conditions that will affect the hemodynamics of the system. This information can be useful to medical professionals and scientists in making decisions for patient care.

1.4 Objectives For This Research

This work is aimed at the development of an experimental system. The design requirements are set by an end-user and those will be the guidelines used throughout the development process. The background for this research is established in the previous sections. This section will lay out the end-user, the requirements, and what is hoped will be achieved.

1.4.1 Identifying the Customer

The customer is what will set the requirements for this work. In this case, the customer is the lab group in which image-based fluid mechanics work is done. While this work focuses mainly on flowing blood through vessels, this will be the main area in which this work is conducted. The lab group works to develop computational models of blood flowing through human vessels, on a non-invasive basis. The models require an experimental method which can validate the computational models.

1.4.2 Customer Related Requirements/Specifications

The objective of this work is to develop a "Pulsatile Circulation Loop" system capable of:

- Mimicking blood flow in human arterial systems
- Reproducing blood flow dynamics in segmented arterial systems.
- Experimental measurement of the blood pressures should be reproduced
- The system should validate medical measurement and computational results
- The system should be capable of measuring patient-specific physiological parameters
- The system should be good for image-based 3-D printed rigid or elastic arteries

This measurement will be done on a patient-specific basis which will allow for a simulation of the physiological conditions present in a patient. The experiment will make use of patient data available from medical instrumentation to create physical vessel geometry using available 3-D printing technology. The resulting printed vessel will be approximately identical to the patient geometric vessel structure. This 3-D printed artery will be mounted into the experimental system with the goal of recreating the flows and pressures seen in the patient data. This experimental system can provide accurate, real-time data on pressure and flow which can be analyzed for parametric components present in the cardiovascular system. These parameters will come from hemodynamics based on the pressure and flow data. The relationship between pressure and flow will be used to provide a better understanding of the properties of the cardiovascular conditions present in each patient. The results from the

experimental system will support concurrent computational fluid dynamics (CFD) studies on the same patient data with experimental results for validation.

The system should be capable of multiple configurations. And will accommodate the variety of geometries that can come with human physiological vessel structure. This may include configurations that contain a single inlet and multiple outlets. The vessel structure may have inlet and outlet geometries that are of significantly different diameters. Because many of these vessels exhibit diseased conditions, they may also be of extensively irregular shapes. These conditions are important as the system will take a patient-specific approach. The system will also be capable of simulating the variety of cardiac cycles in terms of beats-per-minute as well as cardiac output (CO) in terms of volume per heart stroke (beat) and volumetric flow rate. The flow rate seen in the cardiovascular system is a product of heart rate and stroke volume:

$$CO = StrokeVolume * BPM \tag{1.1}$$

The system should also be capable of matching the phases of the cardiac cycle which occur during the contraction of the heart at each beat, as well as the relaxation period as the heart recovers. The period of each phase can vary for each patient. The system will be capable of real-time pressure and flow measurement. Data acquisition will also be used to capture output from multiple channels simultaneously. The data files can be used to determine the system parameters in question, such as systemic resistances, and vascular compliance. The output can then be compared to the patient data as well as the CFD data for further validation.

Several of the concepts were already in place, the development of this system is a further development of the previous work.

1.4.3 Similar Systems in Current Use

There are similar systems in terms of representing the human cardiovascular system through mechanical means. Many of these systems are implemented as a support system

to recreate cardiovascular function to test devices such as left ventricular assist devices. These can give support without the use of animal testing or as training tools. One such device is the Vascular Bioreactor (Aptus Bioreactors, Clemson, SC), which similarly uses valves and reservoirs to be "fully tunable to a range of cardiovascular conditions". While this system contains many similarities, customer requirements will guide this work towards the development of a system to reach the objectives of supporting computational models. The stated objectives will allow for the measurement of pressures and flows in 3-D printed vessels, which can be used in the assessment of stenotic lesions in vessels that can impede the flow of blood to organs and tissue.

1.5 Trans-Stenotic Gradient & Fractional Flow Reserve

The collection of the pressure data will be useful in allowing researchers to approximate such indices as the Trans-Stenotic Pressure Gradient (TSPG). Which is a measurement of the differences in pressure observed across a stenotic lesion. As represented in Fig. 1.5 (top) and defined in Eq 1.2a.

$$TSPG = P_a - P_d \tag{1.2a}$$

Another index which could be a useful measurement tool is the Fractional Flow Reserve (FFR) which uses the pressures from Fig. 1.5, (top). This index is a measurement of the severity of a stenotic lesion, which is done by the ratio of the distal pressure to the proximal pressure. This index is defined in the following relation Eq. 1.2b:

$$FFR = \frac{P_d}{P_a} \tag{1.2b}$$

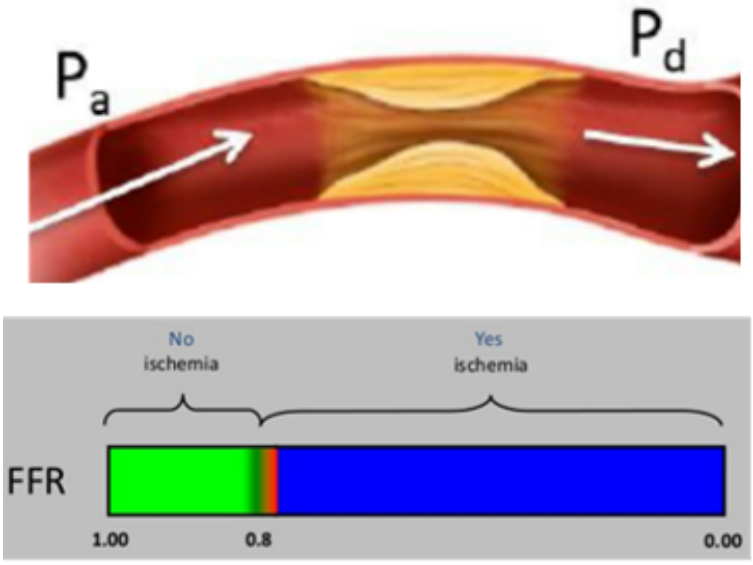

Figure 1.5. Fractional flow reserve (FFR) – Pressure values evaluating Stenotic Lesions using FFR, Eq. 1.2b. Another parameter used to evaluate is Trans-Stenotic Pressure gradient in Eq. 1.2a. Evaluation of FFR can identify possible ischemia. IMAGE: (top) [19]
(bottom) [20]

This relation expresses the flow through a stenosed vessel compared to that of a healthy one. The ratio takes the pressure at the outlet (distal) of the stenotic choke point to the inlet pressure (proximal). A ratio closer to 1.0 is ideal, with the lower limit set at 0.8. This indicates that the pressure drop across a stenotic lesion is 20%. A ratio lower than 0.8 a more significant stenosis, which can indicate ischemia in a vessel. This ratio is considered the "Gold Standard" in evaluating the severity of a stenotic lesion.

2. DESIGN OF EXPERIMENTAL SYSTEM

The design of the experiment is rooted in the Windkessel model. This model is used to simplify the physiological process of the cardiovascular system (CVS) to better understand the function taking place. It uses mechanical components to simulate the physiological functions of the cardiovascular system. Modeling the hemodynamics of the CVS, the relationship between blood flow and pressure can be explored. One physical manifestation of this model can be the Pulsatile Flow Loop.

2.1 Pulsatile Flow Loop Experimental System

This section will describe the pulsatile flow loop - experimental system. The loop is composed of mechanical components that make up the system. The system makes use of mechanical functions to substitute for the physiological mechanics of the cardiovascular system. These system functions contribute to the relationship between pressure and flow. This relationship can be described using the parameters of resistance and compliance. The first section will focus on the key components and how they relate to the cardiovascular system and what role each will play in simulation. The second section will focus on relating the flow and pressure using the Windkessel model. Each component will be described as to its function in cardiovascular flows and its effect on the relation to blood pressure. Each parameter is represented by electrical components which are related using an electric circuit analog that will describe the inlet and outlet conditions of the vessel under investigation. Each inlet and outlet will be related using this circuit.

2.1.1 Pulsatile Loop Set-Up and Measurement

This section will focus on the experimental setup and the flow of the physical system. The system is modeled as a physical Windkessel model, arranged and displayed in Fig 2.1. The system features mechanical components for facilitate the simulation. Additionally, this will include the points of data acquisition throughout the system as well as the reasoning for data collection at any point. The software setup will also be described as it plays an active

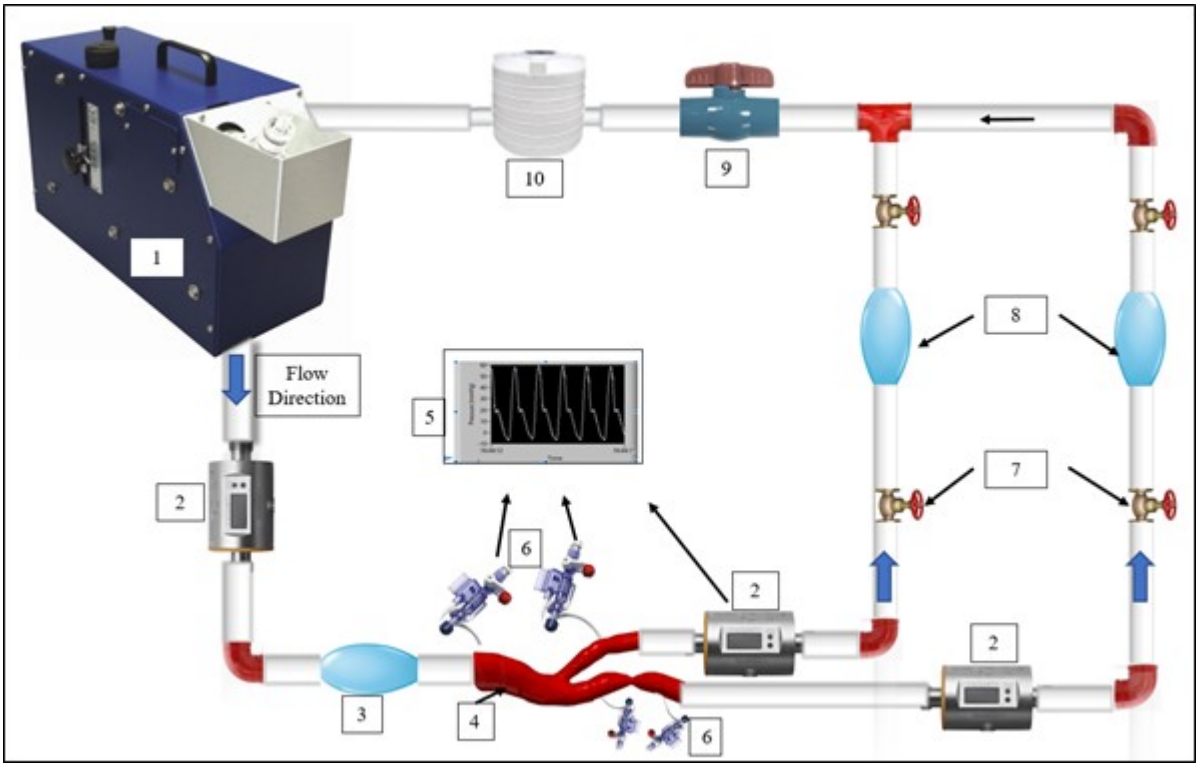

Figure 2.1. Pulsatile Flow Loop Diagram – The system is arranged as displayed above with the components listed. The components of the flow Loop are laid out as displayed in Fig. 4. These components are as follows: 1. Harvard Apparatus Pulsatile Blood Pump, 2. IFM Efector SM-6004 Magnetic Flow Meters, 3. Proximal Compliance Element – Compensating the compliance of the Aorta, 4. 3-D Printed Iliac Artery, 5. LabVIEW Software and Data Acquisition Module, 6. Deltran Pressure Transducer., 7. Local Resistance Valves, 8. Local Compliance Chambers, 9. Peripheral Resistance Valve, 10. Venous Return Reservoir

role in the several key aspects of the experimental setup. An itemized bill of materials is placed in appendix A for reference.

The diagram above (Fig. 2.1) displays the layout of the Pulsatile Cardiovascular Loop. While Fig. 2.2 displays the layout of the experimental system as is present in a lab setting. The experimental set-up considers minimizing abrupt elevation changes. It also considers sharp turns in the flow tubing. Both scenarios are not ideal for maintaining the capabilities of the system without unnecessary resistance.

The components are assembled using a flexible silicone-based high strength tubing, Versilon SPX-50 (Saint-Gobain SA, Courbevoie, France). The tube is designed specifically for

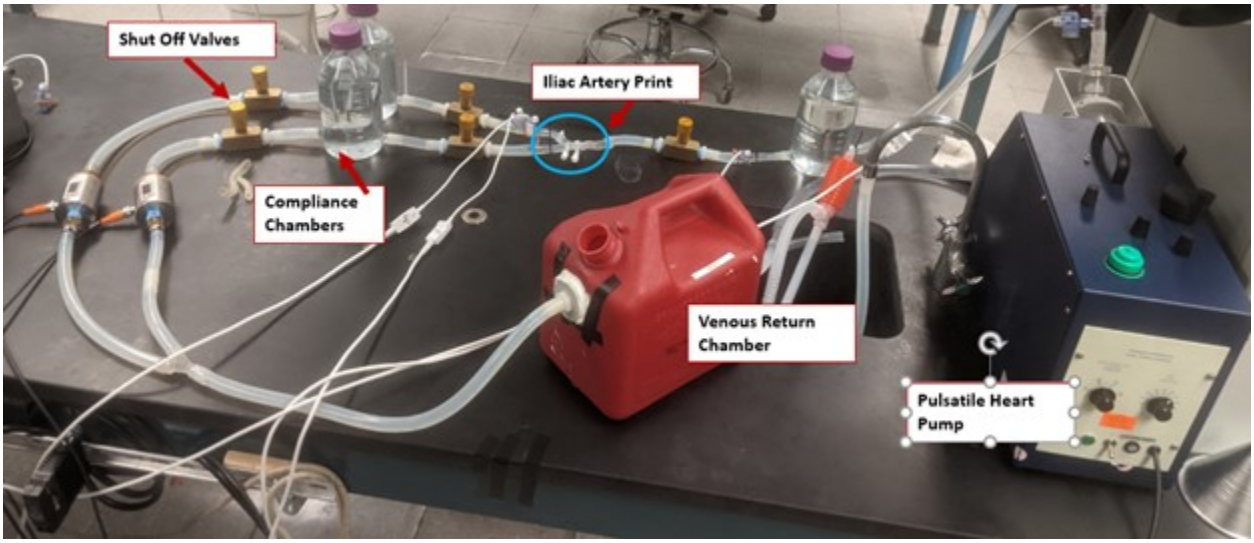

Figure 2.2. Experimental Pulsatile Flow Loop - Represents the Physiology of the Cardiovascular System through Mechanical Components

use as a fluid transfer conduit, generally for use in food, and instrumentation. This material has a Young's Modulus value of 1.71 MPa. In comparison, the arteries of the human body can have a modulus of between 0.4-1.6 MPa [4],[21]. The availability and durability of this material made it an attractive option. While it will influence the pressure-flow relationship due to the flexibility of the tubing, its contribution will be considered negligible when compared to other components, such as compliance. The length of the tube used in each branch will affect the resistance, as per the relation in Eqs. 2.1 & 2.4. This will be considered when constructing each branch and the length between inlet and outlet. Additionally, it is important to maintain a realistic length in terms of human physiology. This will be considered when setting up the experiment.

Additional considerations will be taken to keep the number of unnecessary bends in the system to a minimum. While the system is inherently a "Loop" it will effectively have some bending. Bends will be placed to avoid sharp bends and changes in direction and elevation which could lead to loss in the function of the pump. This could have the effect of artificially increasing pressure where it is not necessary and reducing the effectiveness of the pump. Furthermore, this could also constrict the flow in a manner that is unintended. This has led to the design of connectors that avoid harsh angles that can negatively affect flow. With

these thoughts in consideration, it may be impossible to avoid every loss in the system. However, care will be taken to reduce loss when possible. The components of the Pulsatile Flow Loop are laid out as displayed in Fig. 2.1 and 2.2. These components are as Follows:

1. Harvard Apparatus Pulsatile Blood Pump
2. IFM Efector SM-6004 Magnetic Flow Meters
3. Proximal Compliance Element – Compensating the compliance of the Aorta
4. 3-D Printed Iliac Artery
5. LabVIEW Software and Data Acquisition Module
6. Deltran Pressure Transducer
7. Local Resistance Valves
8. Local Compliance Chambers
9. Peripheral Resistance Valve
10. Venous Return Reservoir

The System Function will occur in the following manner:

The experimental process begins with the Harvard Apparatus Pulsatile Blood pump. The internal mechanism of the pump will oscillate to drive a piston, which begins the flow into the the Versilon silicone tubing. The pump is placed in a manner that minimizes elevation change. This will reduce the loss in pump work due to gravity. The flow is measured directly at the pump outlet to establish the flow rate in the main inlet artery. Directly distal to the flow meter at 2, is the Proximal Compliance element at 3. This initial compliance chamber will act to decrease the water hammer effect caused by pulse wave as it enters the system. This phenomenon causes a bouncing effect in the pressure reading and can distort the pressure results. The compliance chamber regulates the flow and provides the compliance that exists in the aorta. The majority of compliance in the cardiovascular system is provided by the larger vessels the aorta and other major vessels [22]. The position of this chamber is solely for this purpose.

Once the flow has been regulated it enters the 3-D printed artery. As this work focuses on the right iliac artery (RIA), it will consist of one inlet, the right common iliac (RCIA), and two outlets, the right internal iliac (RIIA), and right external iliac artery (REIA). This case features a severely stenosed right external iliac artery. Measuring trans-stenotic pressures can be accomplished by pressure transducers mounted directly proximal and distal to the vessel point with the reduced lumen, where the stenosis is located as displayed in Fig. 2.3.

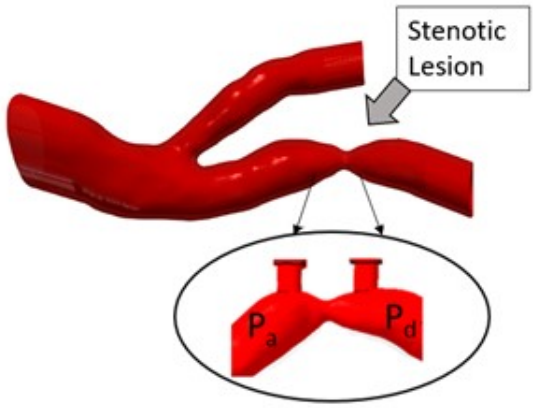

Figure 2.3. Experimental Pressure measurement across a Stenotic Lesion with mounting point for Pressure Transducers in the Iliac Artery

By placing the transducers as close to the choke point as possible, the most accurate pressure values can be taken. Additional pressure transducers can be placed at the right common iliac inlet, as well as the external iliac outlet (6). Each outlet branch will be fitted with additional IFM flow meters, as well as a local resistance valve (7), and local compliance chambers (8). Distal to the compliance chambers, optional resistance valves can be placed to further regulate the flows at the chamber outlets. As the two separate channels are once again brought to confluence, they pass through one final resistance valve (9). This valve is set in place to regulate the resistance of the entire system. It represents the resistance of the peripheral circulation of the micro-vasculature. The aggregate resistance of this set of micro-vessel composes the majority of systemic resistance [23]. This is represented through the relation shown in Eq. 2.4 where the radius to the fourth power is inversely proportional

to the resistance. The final component of the circulation loop is the venous return chamber, which acts as the return chamber, as well as storage for additional fluid. This additional fluid is necessary to ensure that changes in the fluid volume of the compliance chambers will not affect the function of the entire system. As the fluid enters the venous reservoir, it can then re-enter the Harvard pump, to begin the cycle again.

The position of the heart pump is an important consideration. The position of the heart pump in comparison to the flow system should be relatively on the same level as the system. The pump outlet is directed upwards at an approximately 45° angle from the horizontal. Furthermore, the position of the outlet is approximately 12 in. (30cm) from the table surface. As the outlet is directed upwards and above the table surface, this can present several problems. With the use of flexible tubing, care must be taken to avoid excessive bends or pinching in the tube, which may unnecessarily restrict the flow. Additionally, the flow must overcome gravitational losses before entering the tube system. By placing the heart pump in a position in which the outlet is at the level of the table surface, gravitational losses can be kept to a minimum. This placement can add to the systolic upstroke in which the peak pressure value can be reached at a measurable temporal gain.

Additional consideration should be taken with the outlet configuration at the venous return. When the outlet is placed at the venous reservoir it should be placed above the water line within the reservoir volume. By doing this the fluid is allowed to empty into an open system. When the reservoir fluid level is above the return, the fluid entering the reservoir must overcome the fluid head pressure from the volume within, which can create additional loss to the system. It is also advantageous to place the outlet at the same level as the rest of the system, this will maintain regular flow to the pump without interruptions. This could require a table with an opening or a sink. This can also make the placement of inlet and outlet at different levels a necessary part of the design of the reservoir.

2.2 Key Components

This section will discuss the components of the pulsatile flow loop. The printed vessel will be discussed, including the method by which it is obtained through image segmentation.

Background detail will be given as to the role the components play in the experimental system. When appropriate, the detail will include the role in the cardiovascular system and how each can affect the pressure and blood flow in the cardiovascular system. In addition to the flow components, this section will discuss the components used in the data acquisition system as well as the instrumentation used to measure the pressure and flow experienced by the system. The bill of materials (BOM) will be listed in the appendix for reference.

2.2.1 3-D Printed Vessel

The 3-D printed artery is composed of a proprietary liquid photopolymer. This material will harden when exposed to ultra-violet light. This process is due to a chemical reaction and will result in the final product, in this case a rigid plastic artery print.

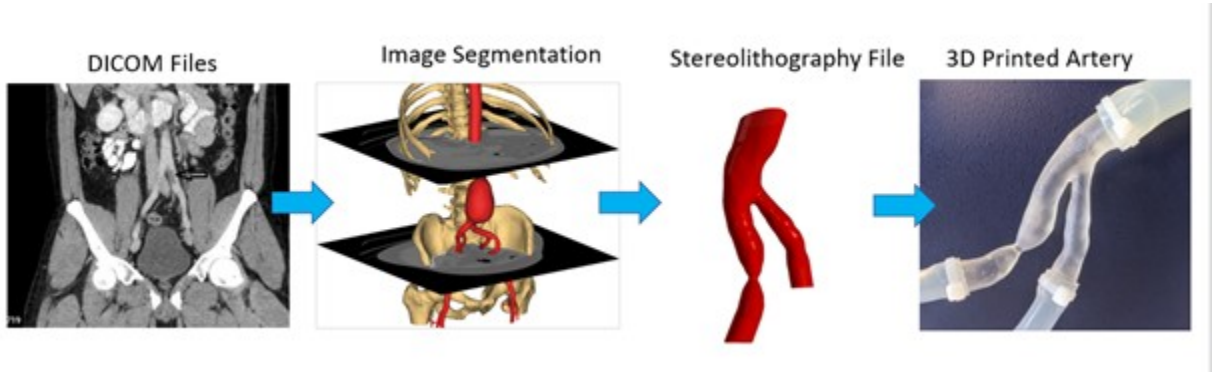

Figure 2.4. Process: Segmentation to 3-D Print. DICOM files are processed to form 3-D images. The image is converted into an STL file, then 3-D printed.

The process of developing a 3-D print of a patient's artery begins with the use of a Computed Tomography (CT) scan, which is acquired from Digital Imaging and Communications files (DICOM). This process combines the images taken from X-rays into a series that are taken from multiple angles. This process, when combined with advanced computing can create cross-sections of "sliced" images of the bones, vessels, and soft tissue of the body.

While this process can be used in many ways, it is quite capable in patients who may have sustained internal injuries. Additionally, it can visualize nearly all parts of the body and identify disease by allowing medical professionals a clearer understanding of the internal conditions of a patient.

2.2.2 Image Segmentation and 3-D Printing

As the patient DICOM data is uploaded into available segmentation software, such as MIMICS Materialise (Materialise NV, Leuven, Belgium), this is displayed in the far left image in Fig. 2.4. The segmentation process is used to isolate the vessel in focus. The files are taken in and assembled into 2-D images. These images are shown from three separate viewpoints. Known as planes titled coronal plane, which divides the ventral and dorsal sections of the body, sagittal which divides the body into left and right portions, and transverse or horizontal planes, which divides the upper and lower potions of the body. As the organ or vessel in scope is identified it can be highlighted. By taking differing views the tissue can be selected in 3-dimensions. As the tissue, in this case, a vessel becomes completely highlighted it can then be isolated and spliced together into a 3-D figure.

The segmented figure can then be extracted and edited to smooth the surface, trim any unwanted edges, or edit inlets or outlets to optimize connection to the system. Once a suitable model has been produced, the file can be converted to 3-D CAD modeling such as a STEP file. The addition of mounting points (shown in Fig. 2.3) for pressure measurement can be done in this CAD modeling stage before the file is converted to an SLA model. The pressure mounts can be placed at any point on the artery where pressure measurement is desired. The 3-D model is then converted into stereolithography (STL) file and then printed using Form3, Stereolithography (SLA) 3-D printer (Formlabs, Somerville, Ma). The printing process produces a 3-D replica of the patient vessel which can be composed of an appropriate material. The rigid 3-D prints are printed using the Formlabs clear photopolymer resin. Resin offering more flexibility and improved elastic properties is available. These prints allow for the investigation of vessel-flow properties in a flexible 3-D print. The properties of the print can be chosen to simulate the flexible properties of real human tissue more closely.

The scope of this study will focus on rigid artery prints. Future studies can introduce more flexible materials, synthetic vessels, or live specimens.

The vessel is mounted into the experimental system connected to the system using a variety of silicone-based tubing (Versilon SPX-50 Tubing, Saint-Gobain Performance Plastics, Akron, OH).

2.2.3 Heart Pump

The heart pump used to drive the system flow is the Harvard Apparatus 1423 Pulsatile Blood pump, (Harvard Biosciences, Holliston, MA) Fig. 2.5. This model is suitable for large animals as well as cardiovascular hemodynamic studies.

Figure 2.5. Harvard Apparatus Pulsatile Blood Pump – Suitable for simulation of the Ventricular function of the Heart in large mammals. IMAGE: [24]

The pump is equipped with adjustable parameters, which can be altered to manipulate the flow and therefore, the pressure waveform. The controls can produce variable cardiac cycles in terms of beats per minute (BPM) ranging from 10 to 100 beats per minute.

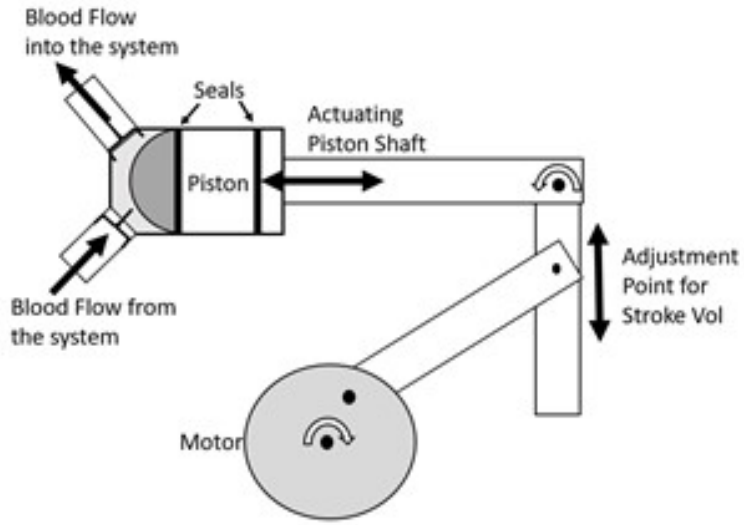

Figure 2.6. Heart Pump internal linkage Design – with reciprocating piston to pump fluid into Pulsatile loop

The cardiac cycle is simulated by a single stroke of the pump which occurs in each cycle. A rotating motor attached to three oscillating arms as displayed in Fig. 2.6. The final link in the linkage chain is a reciprocating piston shaft attached to a piston head. The piston head reciprocates within a cylinder. The cylinder inlet-outlet configuration consists of two one-way valves, one inlet, and one outlet valve. Fluid (water, blood substitute, etc.) enters the cylinder chamber through one valve and is ejected through the outlet valve. The length of reciprocation can be adjusted, which leads to a larger volume that can be ejected from the pump. This action of adjusting the reciprocation travel can vary the volume (taken as cylindrical volume, this motion adjusts the length or 'h' in the cylinder volume, πr^2 h. This volume ejected with each stroke, is known as stroke volume (SV). This simulates the injection of blood from the left ventricle (LV) into the aorta. The Harvard pump contains an adjustable stroke volume (SV) with a range of 15 ml to 100 ml per stroke. The period

of the cardiac cycle is altered by the "beats-per-minute" controls. Altering the number of beats that occur in one minute, the period for one cycle is also altered. This has the effect of increasing the flow rate, by increasing the number of strokes that occur for each minute. As the piston drives the fluid flow and begins each cycle, the volume of each beat is injected into the system at varying rates. As stated in Eq. 1.1, the product of stroke volume per beat and the beats per minute is the basis of volumetric flow rate.

Flow Rate: SV x BPM (Beats per Minute) = Flow rate

Given the flow rate capability and the possible stroke volume the pump is capable of a minimum flow rate 150ml per minute and a maximum flow rate of 10L per minute. The flow rate has the effect of altering pressure as well. Pressure changes will be apparent with each change in flow rate. The change in pressure will be affected by multiple factors within the system. This will be the basis of the pressure-flow relationship that will be referred to throughout this work.

The cardiac period is composed of multiple components. The two main components of this cycle are systole and diastole (Fig. 2.7). Systole is the period of cardiac contraction; the injection of the stroke volume is simulated during this period by the pump stroke. During this period, blood is injected into the aortic arch due to the contraction of the left ventricle (LV). This is the beating of the heart that a person feels. The onset of the systolic phase begins the cardiac cycle.

The slope of onset of systole is a measurement of the systolic slope as it approaches systolic peak. This is a useful parameter [26] and the heart pump should be able to match the upstroke time during systole. Matching the upstroke time can be affected by the placement of the heart pump, which has demonstrated loss due to factors such as gravity. The period of diastole is defined as the period during the cardiac cycle during which the heart relaxes and returns to its original state. The diastolic period is characterized by decay in the pressure waveform until the system is returned to begin the subsequent cycle. As the system returns to the state of relaxation, the cardiac cycle is complete and will begin again. The length of time for each phase is considered in the phase ratio and can be controlled by the cardiac

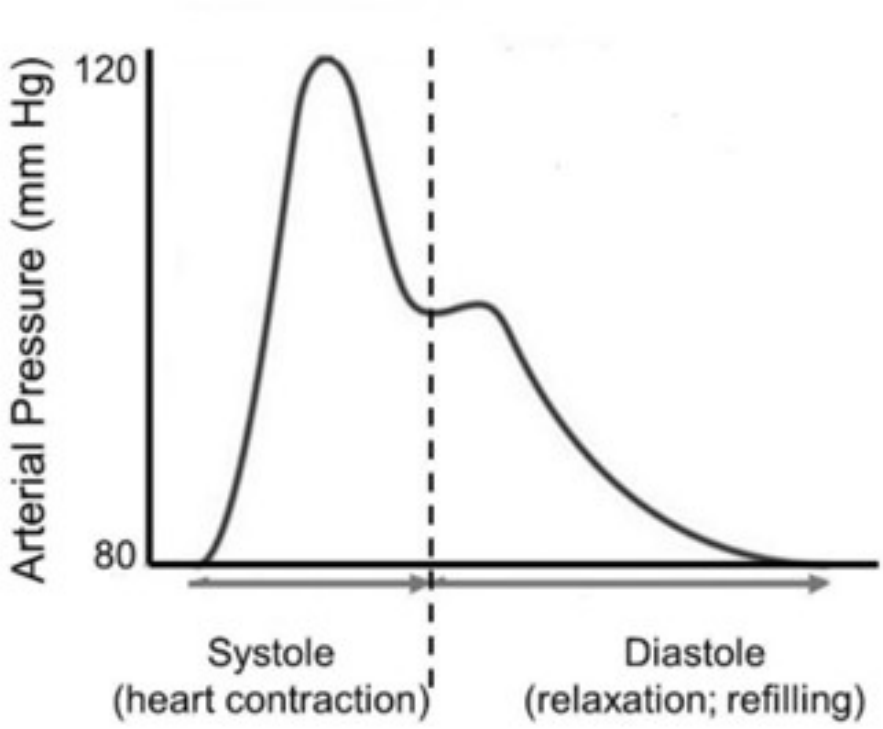

Figure 2.7. Components of the Cardiac Cycle – Systole is phase of contraction of the heart cycle; Diastole is phase of heart relaxation. IMAGE: [25]

phase ratio control on the heart pump. As this ratio controls the length of time in each phase, it can also influence the shape of the cardiac pressure waveform. Specifically, the location of the maximum pressure at the systolic peak. The combinations that are possible on the pulsatile blood pump range from 25/75 (Systole/diastole), 35/65, 45/55, and 50/50. The pump simulates the changes in phase ratio by taking the cycle period and distributing the phases accordingly. As an example, a cardiac cycle of 60 beats per minute, will have a single heartbeat (pump/piston injection stroke) per second. At each stroke, and at a phase ratio of 50/50, 50% of each cycle period will include the systolic period and 50% diastole. This is accomplished by the motor revolution regulating its angular velocity in accordance with the phase ratio, as the piston will move an identical length for each phase. However, varying velocities for a phase ratio of 35/65 (systole/diastole) will require the oscillating shaft to accelerate during the systolic injection phase and to decelerate during diastole, as the system recovers.

In a resting state, the systolic cycle of a typical heart will take place in approximately 1/3 of each cardiac cycle period. With the diastolic period composing the remaining 2/3 of the cardiac cycle [27].

2.2.4 Resistance Valves

Vascular resistance is the resistance to the flow that originates from the vessel geometry. It is a function of the length of the vessel segment, the vessel diameter, and viscosity of the fluid. This can be seen by combining the laws for electrical circuits with the laws for observing flow through pipes, known as the Hagen-Poiseuille equation. In this equation, the vessel resistance is inversely proportional to the radius to the fourth power as shown in Eq. 2.1 and 2.4. [14]

$$\Delta P = \frac{8\mu l Q}{\pi r^4} \tag{2.1}$$

The pressure gradient is further related to resistance through ohm's law. Electrical theory poses Ohm's law as Eq. 2.2:

$$V = IR \tag{2.2}$$

Where the voltage across the resistor, V is equal to the product of current and resistance. The voltage corresponds to the pressure drop, Δp measured between any two points in the vascular tree. Further expansion of the analogy will give the current, I, as the blood flow rate, Q through the vessel.

$$\Delta p = QR \tag{2.3}$$

Which can be combined with 2.1 and rearranged to determine a value for resistance, R.

$$R = \frac{8\mu l}{\pi r^4} \tag{2.4}$$

It can be observed from Eq. 2.4 that resistance (R) is inversely proportional to the vessel radius, to the fourth power. This is demonstrated in Fig. 2.9 where the resistance increases as the valve is closed further. This can infer that any reduction in the vessel lumen will increase in the vascular resistance as well as blood pressure.

The resistance is applied in the form of shut off valves. The valves restrict the flow through the network. The valves are graduated from 0 to 10, and further containing five color-coded bands allowing for up to 50 resistance settings. By considering the equation for resistance, it is clear the vessel radius will be the most influential parameter. Valves are added at each outlet branch as well as at the distal segment just before the venous return reservoir.

Figure 2.8. Resistance Valve – With graduated variation Settings of Closure to vary the resistance in each branch

This distal valve sets the simulated peripheral resistance and will affect the pressure of the entire system. This can be seen as the entire pressure waveform will shift in an upward direction, this will occur for pressure in all branches simultaneously. Local valves will affect each branch on a local level and are analogous to the local geometric conditions which may only have an effect locally. While the effect of changing valve settings in each branch will be noticed elsewhere in the system, their effect is negligible. Valve settings are not specifically associated to any specific resistance value. Changes in valve setting will be more closely related to the flow-pressure relation. The relation is exponential, as is noted by the resistance equation. Due to this relationship, the valves are most effective as they are closed further. This is analogous to the reduction in the lumen radius or the resistance from the peripheral vascular bed.

The resistance valves will have the effect of increasing the pressure in the system. The proximal resistance valve will generally affect the pressure locally. This will be noticed in the pressure in other PTs, especially in upstream branches. Similarly, the peripheral resistance valve will have the same effect, however, the pressure will increase throughout the system.

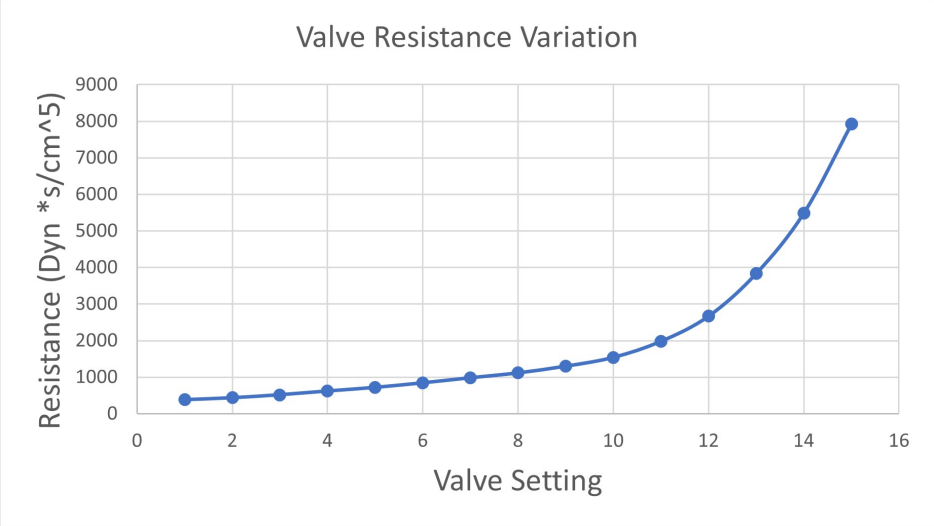

Figure 2.9. The resistance increase at a higher rate as the opening becomes smaller.

The relation between valve setting and resistance shown in Fig. 2.9 is given by Eq. 2.4, where the resistance is inversely proportional to the radius to the fourth power. This is show in the figure using the valve markings as the metric by which the closure is measured. The valve setting is set as a percentage of closure ranging from 34 % - 58% (1 = 34% and 15 = 58%) based on the number of valve settings. The calculated resistance, based on the relation in Eq. 2.3, is given as a function of the valve setting.

2.2.5 Compliance Elements

Arterial compliance is a measurement of vessels to distend. As the left ventricle (LV) ejects blood in the aortic arch, the arch is distended as the pressure increases, and the corresponding volume increase will determine compliance. As the contraction of the LV ends the aortic valve closes. As this signifies the end of the systolic period, the diastolic period begins, and the distended aorta arch releases the excess blood volume into the descending aorta. In the blood pressure waveform, this is signified by the dicrotic notch, which is shown at the dotted line in Fig. 2.7. The compliance in a vessel will determine the rate at which the aorta is released and thereby, its volume of stored blood. The smooth muscle relaxation within the artery wall can have an effect on the compliance and distensibility of a vessel, additionally, the can affect the pulse wave velocity (PWV) [28]. The value of compliance in a vessel is signified by the following relation Eq. 2.5:

$$C = \frac{\Delta V}{\Delta P} \tag{2.5}$$

In the Windkessel model, the compliance shows the effect of the "Air chamber", where the intermittent nature of the cardiac cycle can be transformed into an almost steady, continuous flow. This is due to the elastic nature of the vessels as they store additional blood volume.

This effect is displayed in Fig. 2.10. Where the heart pumps blood volume into the aorta, which expands. This expansion allows it to function as a storage system. The larger vessels are capable of the largest storage capacity, due to their size and ability to distend further. The

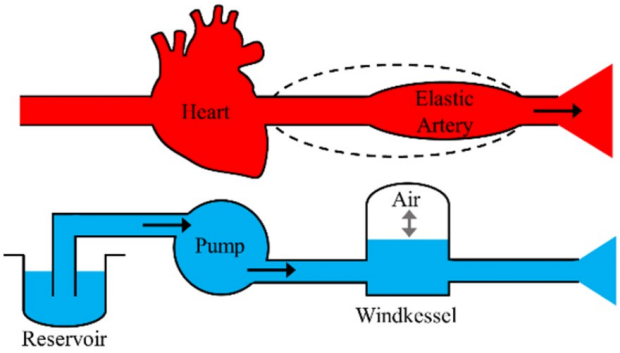

Figure 2.10. Windkessel Effect – Displays the expansion of the Aorta as blood volume exits the heart. IMAGE: [29]

mechanical analog for vessel compliance simulation used in the pulsatile flow loop is in the form of simple air/water chambers. Other concepts for compliance components can take on more elaborate designs such as using elastic membranes or springs. The membrane concept differs from the air/water chamber in that the compliance is regulated by the elasticity of the membrane as shown in Fig. 2.11. While this is a more complex method and has a similar effect of simulating compliance, it is not as simple when changing the compliance. The membrane must be replaced with a membrane of a more suitable elasticity, which will change the compliance.

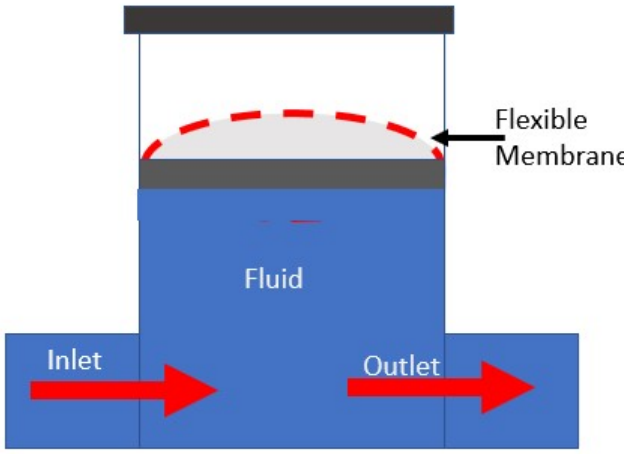

Figure 2.11. Compliance Element Membrane Concept – Flexible membrane provides compliance.

Other approaches involved using a balloon as the expanding entity, which appears to be a more elaborate expansion of the membrane concept.

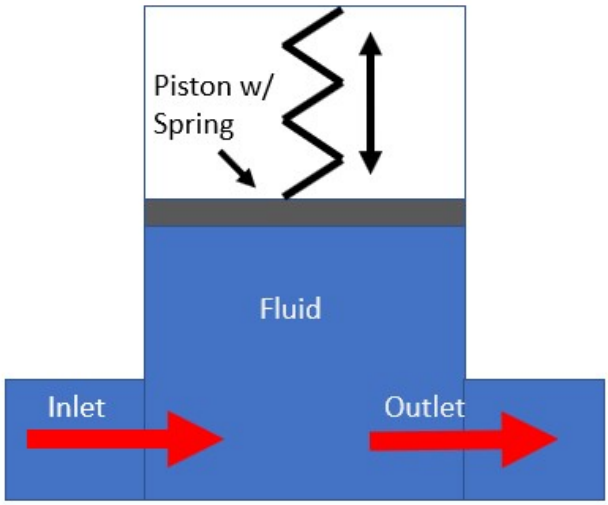

Figure 2.12. Compliance Element spring concept – Oscillating piston compresses a fixed spring. Spring K-constant provides compliance

A spring concept is shown above in Fig. 2.12, in which the spring constant, k, would govern the compliance was another concept that was considered; however, this approach is similar to the membrane the variation of compliance would remain relatively consistent. The gas/liquid chamber approach, Fig. 2.13, requires that only gas and a fluid are necessary, and the change of compliance from each chamber requires only the change in the gas/liquid ratio are varied. In the experimental phase, the ratio is established as a percentage of fluid in the chamber. Once the pressure-flow relationship is established, a more suitable value for compliance can be determined.

Figure 2.13. Compliance Air Chamber – Variable Compliance by water volume. This chamber has a total volume of 2500ml, this chamber has a fluid volume of 1900ml. Taken as a ratio of 0.76.

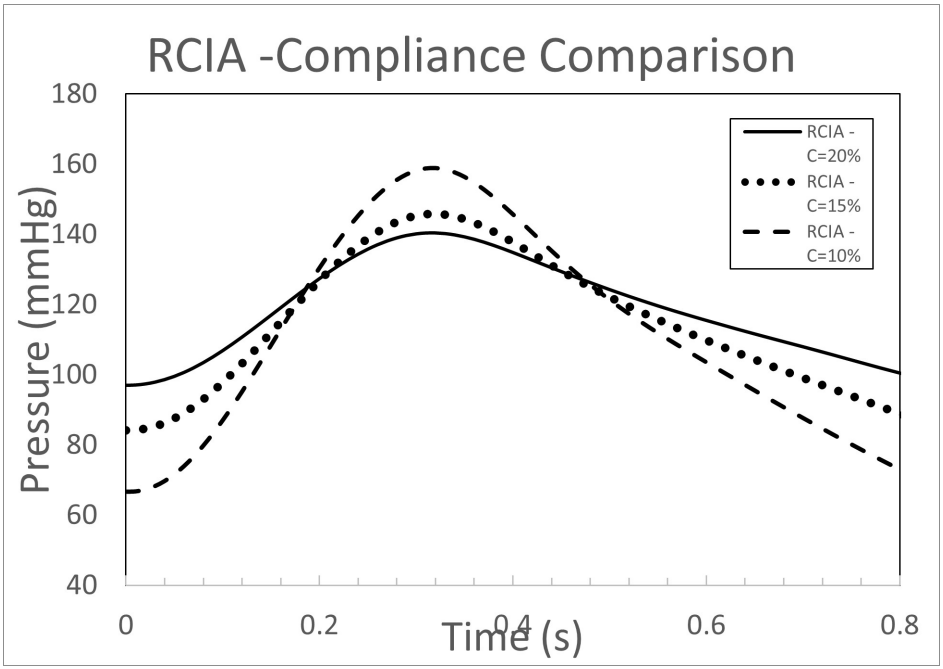

Figure 2.14. Varying the compliance in the chamber by altering the gas/fluid volume. This will alter the pulse pressure in each.

As the chamber is filled with more water, the compliance provided by the chamber reduces. This has the effect of increasing the pulse pressure. This is shown by the relation in Eq. 2.5. By injection of the same volume, a chamber with less compliance will result in a greater ΔP, shown in Fig. 2.14, this is from the relation for compliance $C = \Delta V/\Delta P$. The compliance is set to contain 10%, 15%, and 20% air volume, with the corresponding pulse pressure displayed in the figure. The smaller pulse corresponds to the largest percentage of compliance.

The system fluid is pumped from the heart pump and enters the conduit tubing. Tubing connects to the compliance chamber inlet. This can be configured to include the inlet and outlet as a direct component in the fluid flow. This concept uses the inlet liquid to interact with the full head pressure within the chamber as displayed in Fig. 2.15.

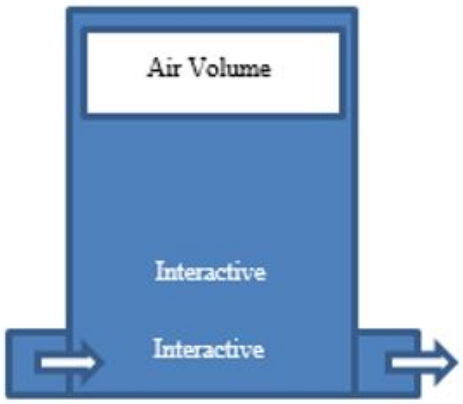

Figure 2.15. Interactive Compliance Chamber – the compliance chamber is an interactive component in the flow. The incoming flow must directly interact with the fluid within the chamber.

A compliance chamber in which the fluid runs directly through the vessel chamber (Known as active compliance), while a chamber which is offset using a more passive concept (T-Shape connector). This is displayed in Fig. 2.16. This configuration has a similar effect although, it maintains the work of the pump with a reduced loss while maintaining the compliance chamber function.

The chamber can vary in shape and size. Compressed air is used as the compression media subject to the pressure applied from the incoming stroke volume and the fluid-gas interface. A larger chamber will inherently be capable of more compliance. Chamber cross-section size will also affect the compliance as the interface area will be larger. The compliance applied to the system at each chamber is regulated by the change of air volume in the chamber. This is described by the combination of the definition for compliance and Boyle's law which states as follows, Eq. 2.6:

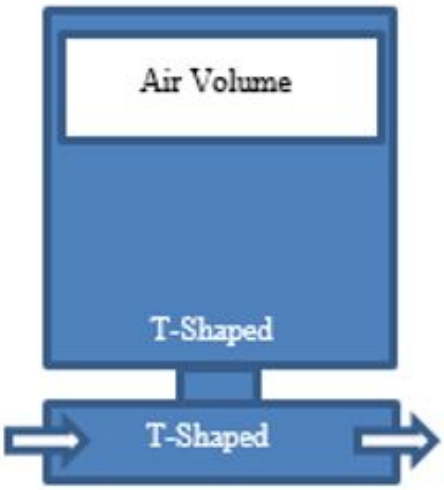

Figure 2.16. Passive Compliance Chamber – the flow is allowed to freely pass with a smaller interaction. This maintains compliance with less stress on the pump.

$$\frac{P_1 V_1}{T_1} = \frac{P_2 V_2}{T_2} \tag{2.6}$$

Where the constant temperature, $T_1 = T_2$

$$P_1 V_1 = P_2 V_2 \tag{2.7}$$

With:

P_1 = Initial Pressure (Atmospheric)

P_2 = Pressure at peak compression

T_1 = Ambient Temp

$T_2 = T_1$

V_1 = Initial Volume

V_2 = Volume at compression

$dV = V_2 - V_1$

The pressure P_2, assumes that the stroke volume has entered before the fluid volume begins to exit the chamber through the outlet. The stroke volume is the difference, dV, between initial volume, V_1 and volume at compression, V_2. As the air volume is enclosed by a simple lid, closed at ambient pressure, the gas is not compressed, and thus the value for the initial pressure is atmospheric. The chamber can be any shape and size that suits the system. The inlet and outlet configurations can vary and is dependent on the application. The location of the inlet and outlets can be set so that the inlet flow does not interfere with the outgoing flow. This can be accomplished by setting the outlet at a slightly higher level that the inlet. This configuration is valid using the interactive compliance method, as the passive concept has only one inlet/outlet, rather than an inlet that is separate from the outlet. Internal pressure of the internal air can also be directly measured using a pressure transducer mounted to the chamber

The compliance of the system has the effect of modulating the pulse pressure. That is to say that the pulse pressure difference, ΔP, between minimum and maximum pressure values will be affected. A vessel system with more compliance will have a smaller pulse pressure, while a more rigid (Less compliant) vessel will have a larger pulse pressure [30]. This relation is given in Eq. 2.5.

2.2.6 Data Acquisition

The data acquisition system (DAQ) is composed of several components designed by LabVIEW (National Instruments, Austin, Texas, USA). The acquisition is separated into two separate data input channels: Pressure data input and flow data input. The data is captured from the system using data acquisition instruments such as pressure transducers and flow meters. As the data these will be discussed in the following two sections.

2.2.7 Pressure Data Acquisition

The pressure measurement in the pulsatile flow loop is done with the use of Deltran® disposable pressure transducers (Utah Medical Products Inc. Midvale, Utah, USA) shown Fig. 2.17. Transducers (PTs) are connected to the system by Luer locks on each connector.

Figure 2.17. Deltran Disposable Pressure Transducers – membrane pressure transducer with Luer lock. IMAGE: [31]

The pressure transducers are individually connected and wired into National Instruments NI-9201, C Series Voltage Input Module. The module measures the input of up to 8 separate voltage signals. The pressure transducers use "Wheatstone Bridge" technology in which the flow pressure is measured by a thin membrane that is in contact with the flow field on one side and to atmospheric pressure on the other. The flow deforms the membrane which expands or contracts. Attached to the membrane are strain gauges which change the electrical resistance which change the voltage output. This voltage signal is captured by the data acquisition system. When processed through a multiplier embedded in the LabVIEW code. This multiplier can be determined through a calibration experiment in which the output voltage is measured using a known pressure. This must be repeated at multiple pressures in order to determine the rate at which the specific transducer outputs voltage. Due to some inconsistency in the pressure transducers, this should be repeated for each individual pressure transducer being used in the experiment. And regularly repeated to ensure consistent measurement throughout the use of the experiment.

The pressure transducers are simply constructed and have an output voltage that is an order of magnitude of 10 µV. Initial tests had proven to be difficult to read the voltage signal produced by the PTs. The signal was consistently minimized by the ambient noise of surrounding electrical components. The solution to this was the construction of an instrumentation amplifier or IN-amp signal amplifier. The In-Amp was constructed for specific use on a standard breadboard. This creates a cost effective, simple approach, which is easily

repaired should it be necessary. The wiring allows for each voltage channel signal, to be individually amplified in order to bring the voltage signal to the forefront of the spectrum.

2.2.8 Flow Data Acquisition

The flow date was acquired using the IFM Efector SM6004 Magnetic-Inductive Flow meter (IFM Electronic, Essen, Germany), Fig. 2.18. These flow meters feature a measurement of flow that is accurate using magnetic measurement with no internal moving parts.

Figure 2.18. IFM Efector SM6004 Magnetic-Inductive Flow Meter – Suitable for flows of lower viscosities as flow is measured without moving gears to be turned. IMAGE: [32]

Initial iterations of this experiment made use of positive displacement flowmeters (PDF). These meters were rated for use with fluids of viscosities in the range of 1-1000 cP. The working fluid used for this work (water: viscosity 1 cP) was at the lower end of the working viscosity range. The design of the PDF meters featured moving internal gearing that required the working fluid move the gears to read flow rate. As the fluid in this project did not have the required viscosity, these flow meters produced unreliable results. Because of this issue, the magnetic flow meters were chosen, since they use a magnetic field to measure flow. The flow meters were connected to the DAQ using the National Instruments NI-9203 C-Series Current Input Module (National Instruments, Austin, Texas). The NI-9203 module measures input current, the IFM flow meters have an analog output signal between 4-20 * 10^{-3} amps (mA). The signal is scalable based on the minimum and maximum flows experienced in the system. In contrast to the pressure transducers, which scale within the LabVIEW code, the

flow meters are scaled on an individual basis for each channel. No instrumentation amplifier was needed as the flow meters provided a suitable signal to be read by the DAQ module.

2.2.9 LabVIEW CODE

The operational code used was developed in LabVIEW (National Instruments, Austin, Texas). This code was used to interpret the input signals captured by the DAQ. The signal from each component group captured by the DAQ is then interpreted by LabVIEW as a signal, current or voltage. The signals are separated into the two components of pressure and flow measurement. While the signal for flow was of an appropriate scale as to be processed directly into the code, the pressure signal, after being amplified, also required the use of a band filter, which filters the signal noise above a level that can allow for only the data signal to be read. Each signal is then grouped into loops where they are further divided into the channels (3-for flow, 3-for pressure) that originate with each measurement device. Within each loop, the signals can be manipulated, with multipliers (scalers) when needed. Each channel can be set to give a visual output in the form of a plot of the pressure or flow data, shown in Fig. 2.20. This can be set to the units that are appropriate for the study. As the signals are received and processed, they are interpreted with a given value. For example, the flow meters are set to output electric current between 4-20 mA. If the flow is known to be within a certain range, between 0.5 ml/min and 4 ml/min, the current can be set to use these values as the minimum and maximum flow rates, respectively.

The data resolution of input signal can be set to an appropriate level by altering the number of data samples to be read as well as the rate (Hz) that these samples are processed. The DAQ system can collect data points at a sampling rate set by the user. A higher data resolution can slow a system with too much data. For this approach, a sampling size of 100 with a frequency of 100/s is chosen. This data can be displayed by the LabVIEW system as a real-time plot which will represent the output of blood pressure during the cardiac cycle. The plots shown in Fig. 2.20 are set to display 5 seconds worth of cycles. For a 1 second cardiac cycle time, this would display 5 cycles, etc.

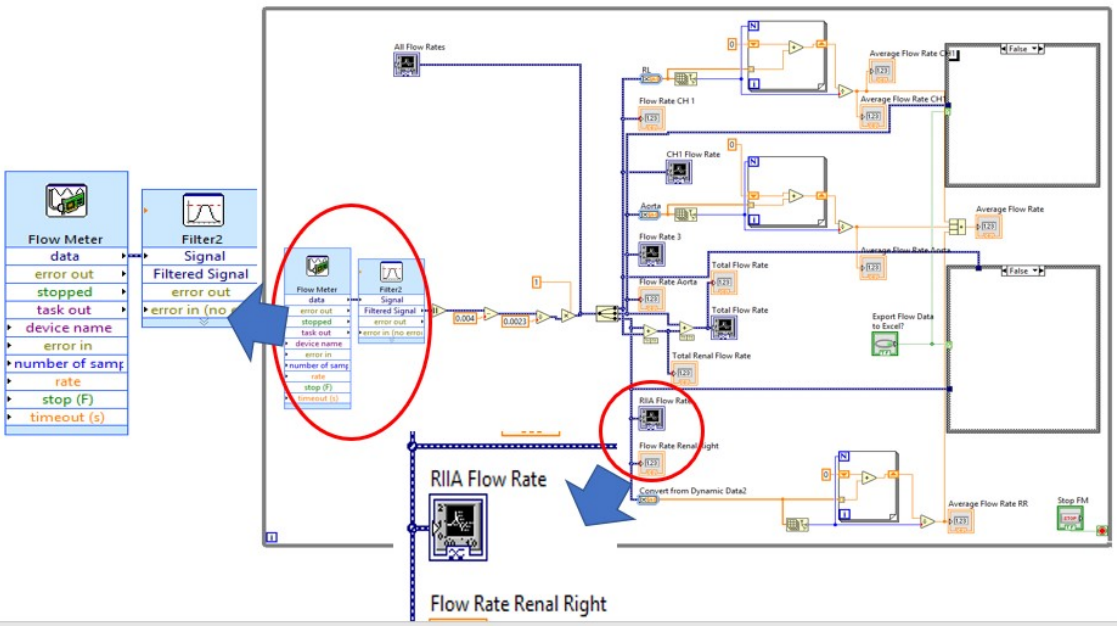

Figure 2.19. LabVIEW code for the Flow data capture – Flow rate is filtered and separated into 3 channels. Multipliers are displayed as floating numbers i.e., 0.0023 used to scale incoming flow signals. The code can produce data in spreadsheet form. Similarly, LabVIEW code for the pressure data is also in use

The LabVIEW code (Fig. 2.19) is also configured to display a rudimentary beats-per-minute monitor. This monitors the peak-to-peak distance. This can allow a researcher the ability to adjust the cardiac time period (BPM) on the Harvard Heart Pump in real-time to match the patient data. The following section will discuss the Windkessel model in detail. Each component of the physical system will be related to the theoretical model. The components' contributions and meaning will be described as well.

2.3 Windkessel Model

This section will discuss the theory used to describe the system. The function of each component of the Pulsatile Flow Loop System will be explained in terms of the math model. Further discussion will include the relation between pressure and flow during each major portion of the cardiac cycle, and how each component will affect the results. The components of the system will be related to the parameters which describe the Windkessel model.

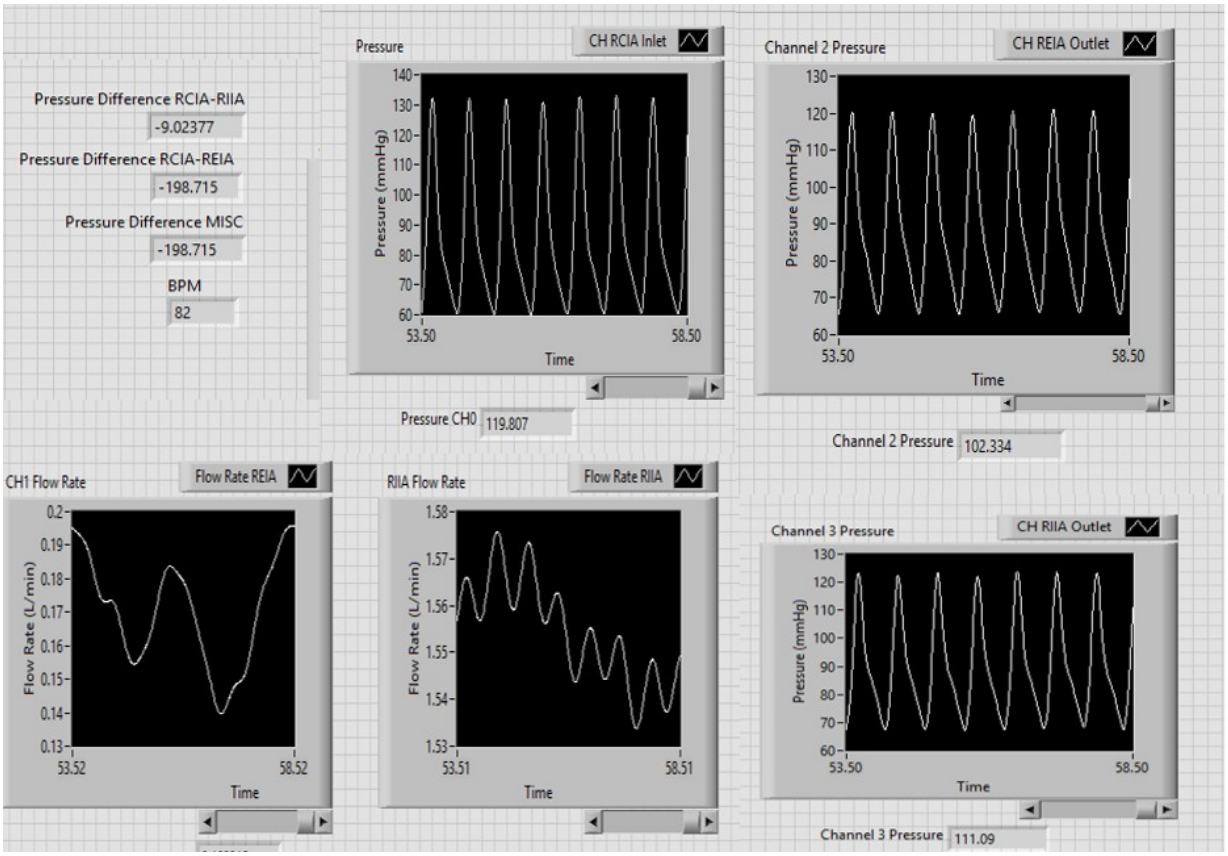

Figure 2.20. LabVIEW Dashboard – Displays the pressure, flow and beats per minute data in real-time. The pressure and flow data plots are set to display up to 5 seconds of data in each window. With a corresponding BPM counter.

2.3.1 RC and RCR Model

The Windkessel model used to describe cardiovascular conditions was originally developed by Otto Frank in 1899. The first model implemented was the 2-elements RC model which defines the arterial system in terms of resistance and compliance [4], [33]. The model makes use of electrical circuit theory such as Ohm's and Kirchoff's law, to describe the flow conditions through each branch of the vessel based on the inlet and outlet boundary conditions. The system can include a simple lumped model, which determines resistance and compliance values for an entire vessel branch. As the two-element model was suitable for representing the exponential pressure decay that can exist in diastole, shown in Eq. 2.8. [34]

$$P(t) = P_0 \mathrm{e}^{-\frac{t}{\tau}} \tag{2.8}$$

Where the t, is time taken at the onset of the diastolic period. The time constant, τ, equals the product of the resistance and compliance, RC. This model can be utilized for estimation of the lumped resistance and compliance taken at diastole, when the flow, Q is zero [34]. This relation can be re-arranged to find Tau, and therefore R and C at diastole. An estimation of the time of diastolic decay must be determined, shown below in Eq. 2.9.

$$\tau = \frac{-t}{ln\frac{P_Dia}{P_Sys}} \tag{2.9}$$

The model was inadequate for describing the flow during systole at the start of the cardiac cycle [4]. Thus, the model can be expanded from a 2-element RC model at each outlet, to a 3-element RCR model that considers upstream as well as downstream (distal) resistance. This can also be modeled as the Characteristic impedance which links the 2-element model to the vessel phenomena, in this case, the wave velocity [4].

The pulse wave velocity (PWV) is a measurement of arterial stiffness between two points of reference[35]. This is influenced by the elasticity and therefore, compliance of the vessel. This can also influence the relationship between the proximal and distal resistances. The PWV travel can associate the wave speed with vessel wall thickness, blood density, and vessel lumen radius. Shown as the Moen-Korteweg relation for PWV in Eq. 2.10.

$$PWV = \sqrt{\frac{E * h}{2 * r * \rho}} \tag{2.10}$$

Where E, is the elastic modulus, h, is the vessel wall thickness, r, is the vessel radius, and blood density, ρ. It will be shown how this parameter can be useful in determining vessel resistances. This relation can be useful in determining the proximal resistances [36].

The boundary conditions at each outlet for the 3-Element Windkessel model. This outlet condition is applied separately at each outlet. The conditions for each inlet can be considered

as stand-alone, however, they will follow the laws for flow conservation. Thus, they can be summed as shown in Eq. 2.13. The resistances, r and R will be discussed in section 2.3.3 and the compliance will be discussed in 2.3.4.

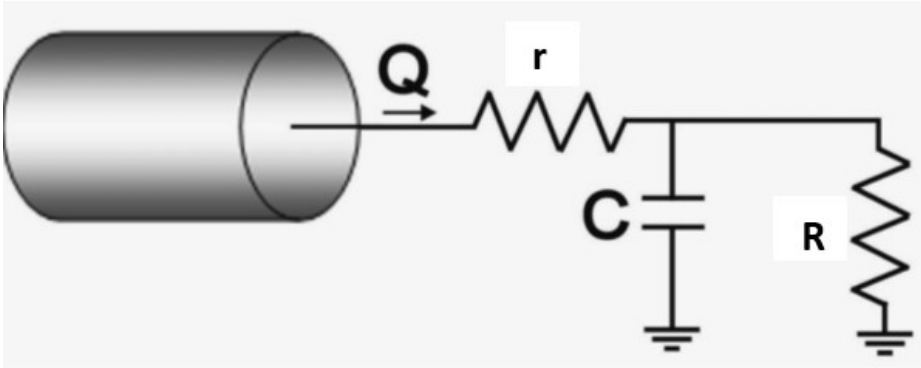

Figure 2.21. 3 Element RCR - Outlet Boundary Condition for each vessel branch outlet. Resistance 'r' proximal resistance and 'R' the distal (Peripheral) resistance. IMAGE: [37]

Wall conditions are non-slip. The working fluid in this case is water. Thus, the standard density for water at standard temperature and pressure will be used. As blood is a non-Newtonian fluid which exhibits shear-thinning behavior in smaller vessels, meaning its viscosity decreases as the shear rate increases [38]. This work will be influenced more by the Newtonian behavior of blood that is present in larger vessels [39].

2.3.2 3-Element RCR

The RCR 3-element Windkessel model (WK3). Which will include compliance from the larger vessels such as the aorta, as well as the resistances present throughout the system. Also, the relationship between the r and R resistances will be addressed, as well as the association to the characteristic impedance in the system. This model will serve as the outlet boundary conditions for each outlet.

2.3.3 Resistances r and R

The resistances in the RCR (WK3) model will be divided into two separate components. The first component is the local resistance, which originates from the geometry of the vessel being investigated. As a stenotic lesion forms, the cross-section is reduced. As is stated in (6), this reduction in radius of the vessel lumen will have an inversely, and to the fourth power, increase in this resistance. The second component of the WK3 model is the resistance that is derived from the smaller vessels, such as arterioles and capillaries. As these vessels are significantly smaller and there are more of them, they add an accumulated resistance in parallel will each other, and in series with the local upstream resistance. This accumulated resistance from the peripheral circulatory system provides the majority of the resistance in the cardiovascular system [23].

The total resistance R_T,in each branch can be determined by peripheral resistance, R, and the proximal resistance, r which can be summed using the summation of resistors in series, $R_T = r + R$. The relation can be further developed by the ratios below [40]:

$$\frac{r}{R_T} = 0.2 \tag{2.11a}$$

$$\frac{R}{R_T} = 0.8 \tag{2.11b}$$

A value for R_T can be determined by rearranging the relation from the Poiseuille law in Eq. 2.3 . This results in the follow:

$$R_T = \frac{\Delta P}{Q} \tag{2.12}$$

Which is developed by the observation of the propagation of arterial pulse waves. This relation can vary which will effect the values of the final resistances. By rearranging Eqs. 2.11a & 2.11b. and combining it with the relation for R_T it can be shown that using this

assumption will result in a ratio of r/R = 0.25. This relation can be useful when determining the values through each branch. As it presents a straight-forward approach to determining resistances.

2.3.4 Compliance

The compliance of the arterial system is a measurement of the vessel's ability to expand and recoil. As the vessel is filled with blood from the heart, it will expand. At the conclusion of the systole period, the volume within the distended vessel will release downstream as the vessel recovers to its original shape. This parameter can be defined as the change in volume ΔV, divided by the change in pressure ΔP. Shown in Eq. 2.5 above.

The relation in Eq. 2.8 can be used to determine the values for r, R, and C. During diastole it is assumed that the blood flow Q has stopped. This is between heart contractions as the heart relaxes. Using the dicrotic notch as the start of the diastolic phase. The pressure at this point can be taken as P_0 and the end pressure, at the end of the cardiac cycle is taken as P(t). The time, t will be the time in seconds from the notch to the end of the cardiac cycle. This can be re-arranged to determine the time constant, τ. Which is equal to the product of peripheral resistance and compliance, τ = RC. This is determined as the natural decay of the pressure waveform materializes. This relation, combined with the relations in Eqs 2.11a, 2.11b & 2.12. Can be used to determine the values for r, R, and C. This is one method of parameter estimation. Other models are available as well, some will be discussed in later sections. Some of these can use the Windkessel model combined with circuit theory to estimate parameters. Which will be expanded further in the next section.

2.3.5 RCR 3 - Element Windkessel Analogy

This section will show the relation between the parameter values in the RCR WK3 model. This will produce the mathematical model which describes the conditions at each boundary. As well as show the flow at the inlet as the sum of the flows. This is displayed in Fig. 2.22. and relation in Eq. 2.13. Where the flow through the common iliac will be divided at the bifurcation of the two branches, from the Right Common Iliac Artery (RCIA), which

bifurcates into the Right External Iliac Artery (REIA) and the Right Internal Iliac Artery (RIIA). The REIA is severely stenosed, which is estimated at 80% reduction cross-section in the vessel lumen.

$$Q_{IN} = q_1 + q_2 \tag{2.13}$$

Where Q_{IN} is the flow rate through the inlet at the right common iliac artery (RCIA). Additional flow rates through each branch of the bifurcation are q_1, for the right internal iliac artery (RIIA), and the flow rate through the right external iliac artery (REIA), q_2. This is shown in Fig. 2.22.

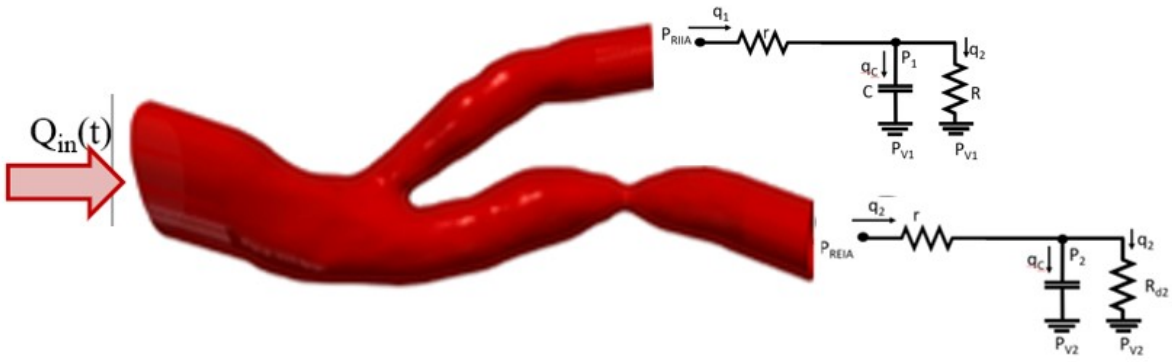

Figure 2.22. Right Iliac Artery – Full WK3 – RCR Outlet boundary conditions Windkessel Model. The inlet Right common iliac artery bifurcates into right internal (top) and right external (bottom) arteries. The REIA is severely stenosed.

This model can be further related by the Windkessel circuit which will represent the entire artery, Fig. 2.23. This follows the same model as Fig. 2.22. with only the electrical circuit analog shown, without the vessel anatomy.

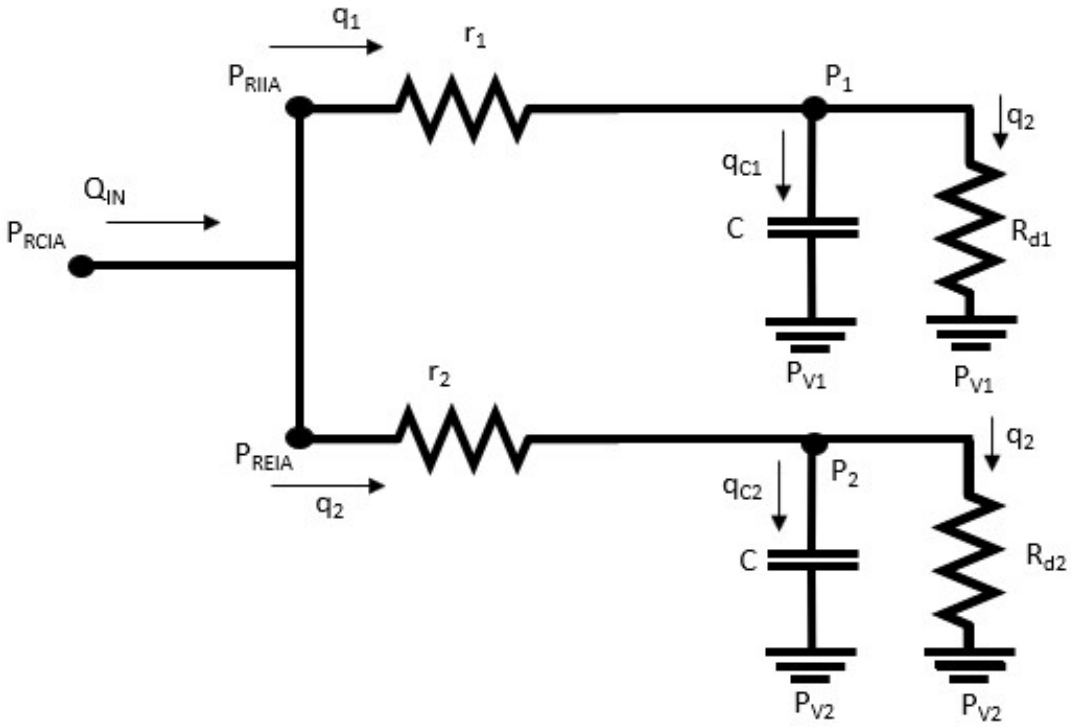

Figure 2.23. Complete iliac artery Windkessel Circuit with RCR in each branch.

The branches are separated into circuits for each artery branch. Shown in Fig. 2.24. This will be the basis for the mathematical model using the outlet boundary conditions in each branch.

The math model further separates the flows into components that are associated with the compliance, q_C and the peripheral resistance, q_2. These components operate in parallel as the two components of the time constant, $\tau = RC$.

$$q_1 = q_c + q_2 \tag{2.14}$$

The flows through each branch are identified using the relations for flow, resistance and pressure drop, for example q_1. The pressure across a resistor, r, between the inlet of the vessel branch (RIIA) is defined by Eq. 2.15:

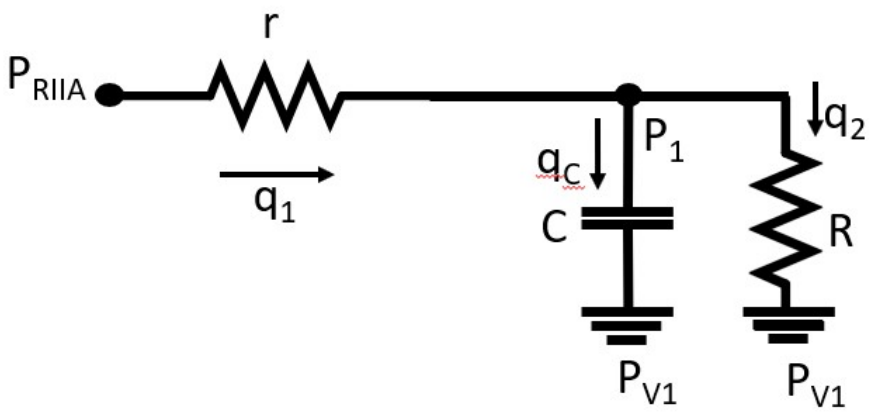

Figure 2.24. RCR model at each branch outlet, this model shows the RIIA vessel outlet conditions. The REIA vessel model will be similar.

$$q_1 = \frac{P_{RIIA} - P_1}{r} \tag{2.15}$$

As the flow passes point, P_1, it can then branch into the components, q_C, the flow through the compliance element, and the flow, q_2 through the peripheral resistor, R. These are related to the flow, q_1 through the relation in Eq. 2.14, q_C, and, q_2 are defined in Eq. 2.16 & 2.18, respectively.

$$q_C = C\frac{dP_1}{dt} \tag{2.16}$$

As stated previously, the pressure in the venous system is significantly smaller than the arterial pressure and can therefore be assumed to be zero. Thus, the flow, q_2 through the peripheral resistor, R can be reduced in Eq. 2.18. The pressure in the venous system is comparatively insignificant when compared to the pressure in the arterial system, the venous pressure can be considered to be zero [34].

$$P_V \approx 0 \quad (Venous) \tag{2.17}$$

$$q_2 = \frac{P_1 - P_V}{R} = \frac{P_1}{R} \tag{2.18}$$

Can be combined and substituted into q_1, Eq. 2.14 which will produce the relation shown in 2.20.

$$q_1 = \frac{P_1}{R} + C\frac{dP_1}{dt} \tag{2.19}$$

Substitution of P_1 re-arranged from Eq. 2.15 to get 2.20 and 2.21

$$q_1 = \frac{P_{RIIA} - q_1 r}{R} + C\left(\frac{dP_{RIIA}}{dt} + r\frac{dq_1}{dt}\right) \tag{2.20}$$

$$q_1 = \frac{P_{RIIA}}{R} - \frac{r}{R}q_1 + C\frac{dP_{RIIA}}{dt} - R_1 C\frac{dq_1}{dt} \tag{2.21}$$

Rearrange to get:

$$C\frac{dP_{RIIA}}{dt} = rC\frac{dq_1}{dt} - \frac{P_{RIIA}}{R} + \frac{r}{R}q_1 + q_1 \tag{2.22}$$

Divide through by C

$$\frac{dp_{RIIA}}{dt} = r\frac{dq_1}{dt} - \frac{P_{RIIA}}{RC} + \frac{q_1}{C}\left(1 + \frac{r}{R}\right) \tag{2.23}$$

After re-arranging and grouping like terms on each side of the equation the value for the pressure, P_{RIIA} can be given by Eq. 2.24 and then finally, Eq. 2.25.

$$\frac{dP_{RIIA}}{dt} = r\frac{dq_1}{dt} - \frac{P_{RIIA}}{RC} + \frac{q_1}{C}\frac{r+R}{R} \tag{2.24}$$

$$\frac{dP_{RIIA}}{dt} + \frac{P_{RIIA}}{RC} = r\frac{dq_1}{dt} + \frac{r+R}{R}\frac{q_1}{C} \tag{2.25}$$

The relations from the equations above can be used to determine the parameter values for compliance and both resistors.

As Eq. 2.8 and 2.12 are evaluated, the relation for r & R, shown in Eq. 2.26. is used to determine resistance R, at diastole and r. Which can be used to find compliance, C for the vessel branch.

$$R_T = r + R \tag{2.26}$$

3. APPLICATION IN ILIAC ARTERY STENOSIS

3.1 Iliac Arterial System

This study focused on the iliac artery, Fig. 3.1. This vessel is located in the upper portion of the leg. The iliac is one of the major vessels in the lower portion of the body. As blood flows through the lower aorta, the abdominal aorta bifurcates into the left and right common iliac arteries. Each of these arteries further splits into the internal and external iliac arteries (RIIA & REIA respectively).

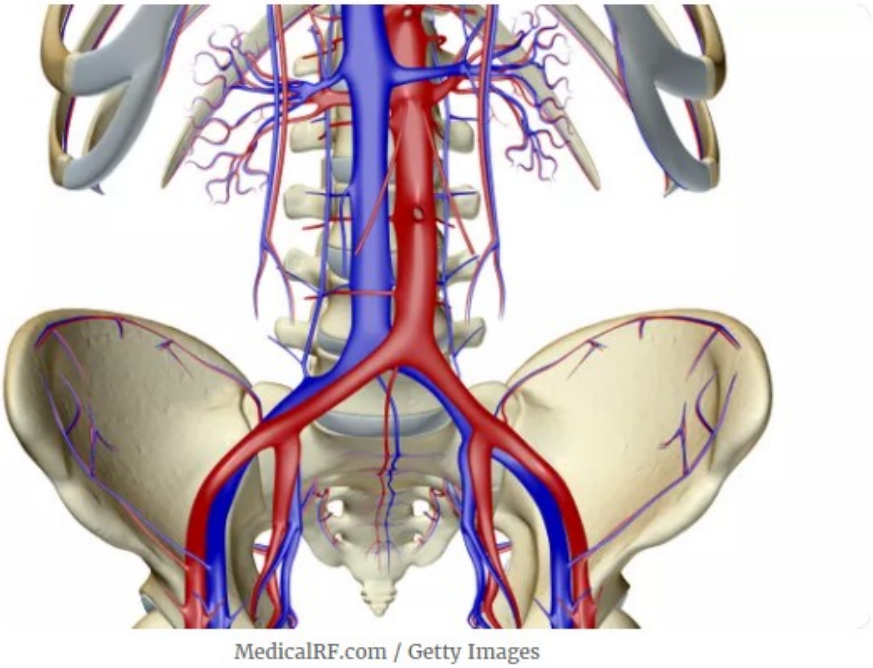

Figure 3.1. Iliac Artery – The main artery which bifurcates to each leg from the abdominal aorta. IMAGE: Getty Images, 2022, Blood Supply of the Pelvis, [41]

Each artery REIA and RIIA supplies blood flow to the lower leg, such as the femoral artery. Further functions of the iliac artery are supplying the lower abdominal wall with blood (REIA) or supplying the pelvis (REIA & RIIA) [41].

3.2 Measurement and Validation

The experimental setting, displayed in Fig. 2.1 & 2.2 in section 2, is the arrangement of the pulsatile loop. The printed artery being studied is the right iliac artery in Fig. 2.22. This vessel consists of a single inlet and two outlets. The right common iliac artery, RCIA, is the branch with the severe stenosis being assessed. A single flow meter is placed at the outlet of the heart pump to measure the flow rate which will enter the vessel. One pressure transducer is placed at the inlet of the vessel. Pressure transducers are also placed at each branch outlet, with a flow meter placed at the same position. Once conditions are established for the system, pressures can be measured with additional pressure transducers placed trans-stenotically. Thereby allowing for measurement of the proximal and distal pressures before and after the stenosis.

The patient data for systolic and diastolic pressures can be used as target pressures when measuring conditions. Heart pump settings are set by the use of patient data, such as heart rate, and by the use of a pre-established flow rate (done by the previous CFD study). Once the initial settings are in place, the system of shut-off valve resistors and compliance chambers can be manipulated and adjusted to reach the desired pressure and flow rate targets.

The validation of the results is done through the comparison of the experimental data to the results from the CFD. In terms of the invasive pressure and flow results, the experimental data can be compared to the pressure plots for each branch as well as the minimum and maximum values. The pressure plot shape, location of the peak pressure in terms of time during the cardiac cycle, and the location of the dicrotic notch can also be useful markers in matching the experimental and invasive results. The CFD results can be useful through the comparison of the parameter, such as the resistance and compliance values. By using the pressure and flow waveform shapes as a benchmark, the experimental results can be further evaluated.

3.2.1 Comparison of Invasive and CFD

The Invasive and CFD results are sourced from patient data and previous studies, respectively. The iliac artery at the center of focus in this study is one of these patients. The

associated patient medical data is also included which is provided by supporting medical professionals. The medical data was used previously to obtain through CFD the parameter results as well as the pressure waveform. This pressure wave is compared to the patient data from the invasive measurement. As the medical data was originally received, it was then processed using the plot digitation method. This method used the original scans of patient data, with available observations such as the minimum and maximum values in the patient monitor data to generate the patient pressure waveforms used for this study.

Figure 3.2. Patient Monitor Data – The basis for the plot digitation for the right common iliac artery. The plots shown in the figure are used to digitize and generate patient data.

This produced the pressure waveform data used as the invasive measurement. The CFD data was produced by a previous study, which produced the flow rate data, in addition to the blood pressure data. In this case, the invasive data for the right internal iliac artery was not provided.

The following plots compare the experimental data acquired from the pulsatile flow loop and to the pressure data from the invasive and the CFD model.

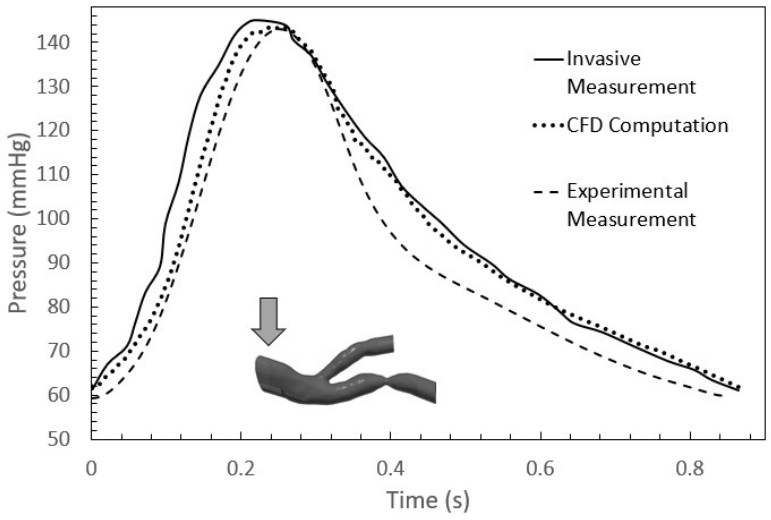

Figure 3.3. Right Common Iliac Artery – Invasive, CFD, and Experimental Data. This artery segment is the inlet for the right iliac artery under investigation.

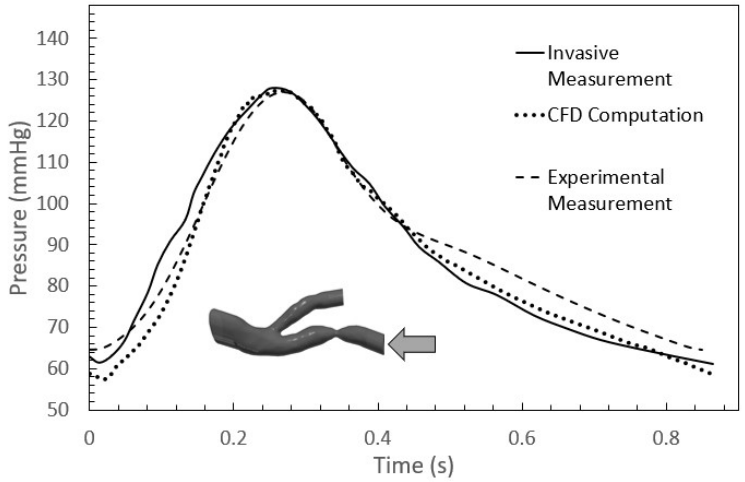

Figure 3.4. Right External Iliac Artery blood pressure comparison between the Invasive, CFD, and Experimental data. The REIA is shown above as a severely stenosed segment. The estimation of reduction is approximately 80% lumen radius reduction.

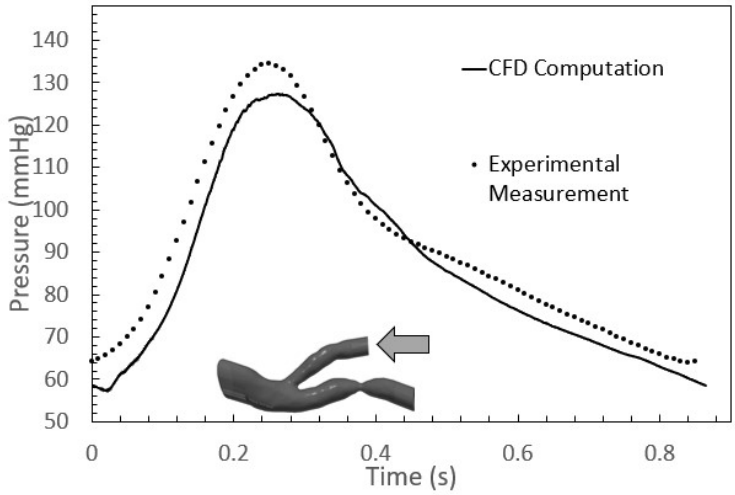

Figure 3.5. Right Internal Iliac Artery – Comparison between CFD pressure wave and the experimental pressure. Invasive data not available.

Table 3.1. CFD and Experimental tabulated Systolic and Diastolic pressures and BPM

	CFD Results			EXPERIMENTAL		
	RCIA	REIA	RIIA	RCIA	REIA	RIIA
P_sys (mmHg)	143.671	127.41578	134.01398	144.148	127.833	136.277
P_dia (mmHg)	61.9174	57.333787	60.303274	59.3414	64.5325	63.932
BPM	69.4262			68.965517		

The pressure comparison for the Right Internal Iliac artery is displayed in Figs. 3.3-3.5. The results can be compared to the invasive and CFD values provided from previous studies. These can also be compared to the values from experimental. The mathematical models use the pressures at systole and diastole, along with the pulse pressure, mean pressure and mean flow values, these will be presented and used to estimate the parameters for each vessel branch. These pressure values are shown in table 3.1.

3.3 Results

The results from the study show a right iliac artery, with significant stenosis on the right external iliac branch. As stated, the stenosis reduced the vessel lumen by approximately 80%. The results will discuss the severity estimation of the stenosis.

3.3.1 TSPG and FFR Results

The following plots will compare the trans-stenotic pressures around the lesion, Fig 3.6 P_a and P_d.

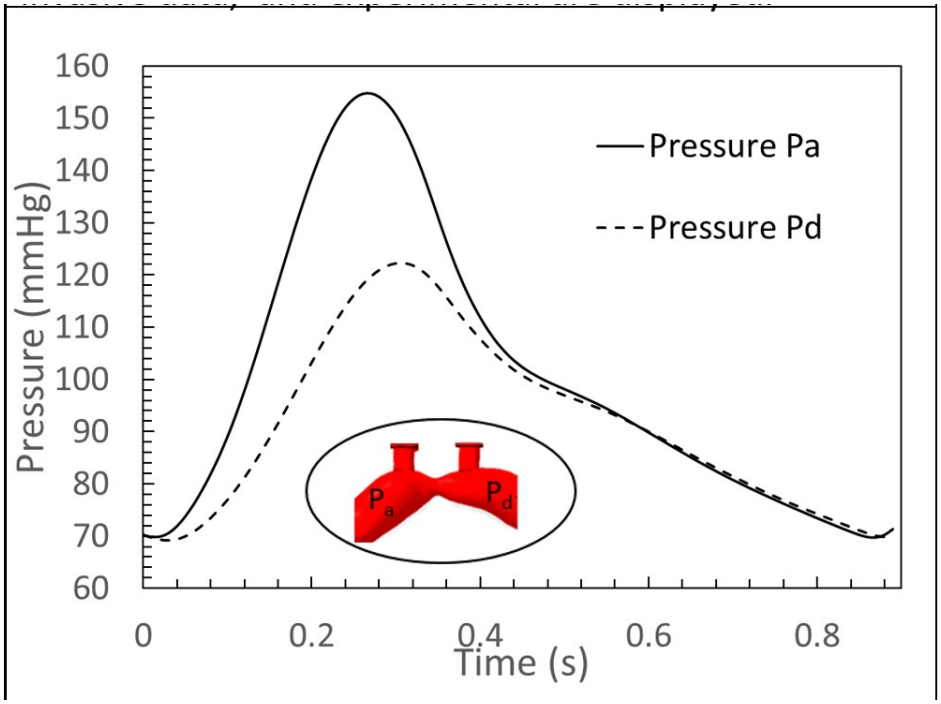

Figure 3.6. The Pressure at stenotic lesion – with Pa, the proximal pressure from the aortic bifurcation and Pd, the distal or downstream pressure in relation to the stenosis. The pressures will be used to determine the Fractional Flow reserve, FFR, and the Trans-Stenotic Pressure Gradient, TSPG.

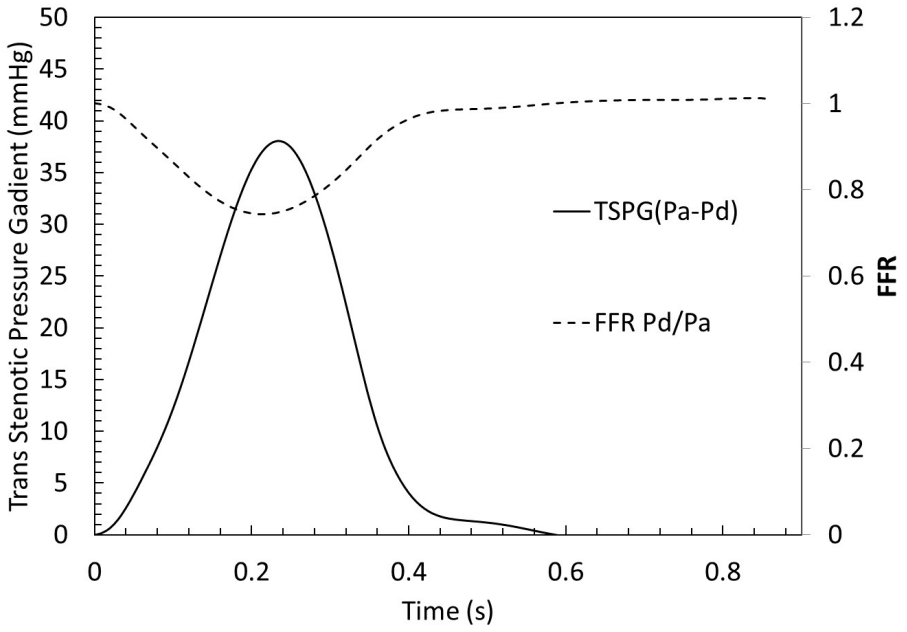

Figure 3.7. Fractional Flow Reserve and Trans-Stenotic Pressure Gradient – These values are used to evaluate the severity of the stenosis.

The results from the TSPG and the FFR, using the relations in Eq. 1.2a and 1.2b, are shown in Fig. 3.7. The plots displayed show the fractional flow reserve to be approximately 79%. This can be interpreted as a 21% drop in pressure. This puts the artery in the region of ischemia. The calculated values are shown in table 3.2.

Table 3.2. Pressure ratio, Fractional Flow Reserve, FFR, and Trans-Stenotic Pressure Gradient measured for the pressures across the stenotic lesion in the REIA

FFR	0.790507703
TSPG (mmHg)	32.416

4. SUMMARY AND DISCUSSION

4.1 Achievements in this Study

The main objective of this work, the development of a working experimental system for measurement of blood pressures in 3-D printed artery vessels has been reached. The system is capable of measuring pressure and flow in the experiment system through a 3-D printed rigid artery. The system allows for real-time data to be observed while in operation. This data can be captured and post-processed using available data processing software. The system can accommodate multiple configurations of vessels in terms of vessel radius, vessel length, as well as the number of inlet/outlets. The system can be used with other vessels of similar scale.

The process by which the 3-D vessel prints are obtained allow for a "patient-specific" study that can determine the parameter values in an individual patient. Further use of this system allows for the support and validation of CFD code simultaneously in development.

Table 4.1. Initial objectives are displayed as completed successfully.

	STATUS	Objective Met?
Should mimic blood flow in human arterial systems	COMPLETE	Yes
Reproducing blood flow dynamics in segmented arterial systems.	COMPLETE	Yes
Experimental measurement of the blood pressures should be reproduce	COMPLETE	Yes
The system should validate medical measurement and computational results	COMPLETE	Yes
The system should be capable of measuring patient-specific physiological parameters	COMPLETE	Yes
System should be good for image-based 3-D printed rigid or elastic arteries	COMPLETE	Yes

Table 4.1 displays the objectives as stated previously. The status of each is submitted and each objective has been met. The system is operational and capable of each of the items listed as parameters.

4.2 Drawbacks and Possible Improvements

While the system proved that the method works, it was not without its limitations. The pump that was implemented had several issues regarding the accuracy of the cardiac cycle, i.e., Beats per minute, the target heartbeat was 12% higher than the heart pump setting. The heart pump was on the "low end" in terms of output at the cardiac upstroke. This was observed at the onset of systole when the pump was incapable of matching the slope increase during systole. This resulted in a small, however noticeable lag in the peak blood pressure of the system. Normally this was observed at 0.02-0.04s, and while the maximum BP was matched with the patient data, the system displayed this lag. The lag was improved upon through several improvements, simple methods such as where the pump was placed, how the compliance chambers interacted with the flow, such as a more passive approach placing the chamber adjacent to the flow, rather than having the chamber take a more direct approach in which the flow passed through the lower portion of the chamber. One final improvement which saw a noticeable difference was the level of the fluid in the venous reservoir. Allowing the venous return to flow into the upper, open part of the container, rather than into a filled container, also showed improvements. This was accomplished by maintaining a water level in the reservoir that was below the return outlet.

The compliance elements in their current state can be somewhat difficult and cumbersome. As the compliance is changed through the volume of the working fluid in the chamber, there is no simple method for changing the fluid level. Chambers are equipped with lids, which, when not tightened fully, can cause a lack of seal, losing airtight capability. During the operation, this tends to change the water level as the pump pushes water into the chamber, pushing air out. This is noticeable when the compliance changes are noticed in the pressure data output. By automating this compliance system, this could be remedied, making its use simpler during operation.

Focus on the artery print dimensions during the segmentation process could be useful. While the general geometry is kept consistent when compared to the in vivo vessel geometry, the printed artery can be slightly inaccurate in terms of dimensions. This phenomenon is especially important to consider when considering smaller vessel conditions such as a severely occluded vessel. As a vessel with a severely reduced lumen is printed, the resulting print can be one with even more reduced or possibly completely closed off.

4.3 Future Works to Advance this Research

Aside from the improvements discussed in section 4.2, the experimental system can be further developed in several ways. Future methods which could add to the impact of this work would be the use of a more accurate heart pump. If possible, the development of a more suitable pump system would be beneficial by creating a customized pump. Perhaps developing the pump to create a more realistic "contraction" on the stroke input that would provide a more accurate systolic upstroke.

The analysis for parameter estimation use the math models described above. This will determine the values for the resistances (R_T, r, R) and compliance (C). The work estimated parameter values should be completed in future works. This will allow for the establishment of an appropriate model.

Future work involving the artery print can also be made. These can include flexible printing resins that offer flexibility. By changing from resin to a flexible or elastic material the experiment can begin to evolve towards a more life-like vessel which could produce more accurate results. Research would be required to find a suitable material which offers the most closely matched material properties. The method for developing the 3-D print would be identical to the method used for the rigid print. Another vessel improvement could be the use of artificial arteries which are available through medical professionals. These are also composed of different materials as well as different designs. These artificial vessels would be mounted similarly and could be compared to other vessel materials.

Finally, this work could be furthered by the use of cadaver vessel specimens. Several considerations would be necessary in terms of mounting, handling, and storage of live tis-

sue. Additionally, this would involve multiple challenges needed to comply with training, regulatory, and legal requirements, their use could provide some insight into the validation of the system as well as useful data from testing done on live tissue. This would indeed add another level of capability as well as an additional point of comparison.

REFERENCES

[1] W. H. Federation, *Cardiovascular disease*, Mar. 2022. [Online]. Available: https://world-heart-federation.org/what-is-cvd/.

[2] G. Mahé, A. Kaladji, A. Le Faucheur, and V. Jaquinandi, "Internal iliac artery stenosis: Diagnosis and how to manage it in 2015," *Frontiers in Cardiovascular Medicine*, vol. 2, p. 33, 2015.

[3] CDC, *Facts about hypertension*, Sep. 2021. [Online]. Available: https://www.cdc.gov/bloodpressure/facts.htm.

[4] N. Westerhof, J.-W. Lankhaar, and B. E. Westerhof, "The arterial windkessel," *Medical & biological engineering & computing*, vol. 47, no. 2, pp. 131–141, 2009.

[5] T. W. Secomb, "Hemodynamics," *Comprehensive physiology*, vol. 6, no. 2, p. 975, 2016.

[6] R. Bolli, "William harvey and the discovery of the circulation of the blood: Part ii," *Circulation research*, vol. 124, no. 9, pp. 1300–1302, 2019.

[7] R. Nave, PhD, *Poiseuille law*, [Apr 2022], 2005. [Online]. Available: http://hyperphysics.phy-astr.gsu.edu/hbase/ppois.html.

[8] M. Rafieian-Kopaei, M. Setorki, M. Doudi, A. Baradaran, and H. Nasri, "Atherosclerosis: Process, indicators, risk factors and new hopes," *International journal of preventive medicine*, vol. 5, no. 8, p. 927, 2014.

[9] Y. S. Chatzizisis, A. U. Coskun, M. Jonas, E. R. Edelman, C. L. Feldman, and P. H. Stone, "Role of endothelial shear stress in the natural history of coronary atherosclerosis and vascular remodeling: Molecular, cellular, and vascular behavior," *Journal of the American College of Cardiology*, vol. 49, no. 25, pp. 2379–2393, 2007.

[10] P. A. VanderLaan, C. A. Reardon, and G. S. Getz, "Site specificity of atherosclerosis: Site-selective responses to atherosclerotic modulators," *Arteriosclerosis, thrombosis, and vascular biology*, vol. 24, no. 1, pp. 12–22, 2004.

[11] Y. Yoshida, T. Yamaguchi, C. G. Caro, S. Glagov, and R. M. Nerem, *Role of blood flow in atherogenesis*. Springer, 1988.

[12] T. Asakura and T. Karino, "Flow patterns and spatial distribution of atherosclerotic lesions in human coronary arteries.," *Circulation research*, vol. 66, no. 4, pp. 1045–1066, 1990.

[13] RWJBarnabasHealth, *Renal artery stenosis*, [Apr 2022], 2019. [Online]. Available: www.rwjbh.org/treatment-care/heart-and-vascular-%20care/diseases-conditions/renal-artery-stenosis/%20RWJBarnabas%20Health.

[14] R. Klabunde, *Cardiovascular physiology concepts*. Lippincott Williams & Wilkins, 2011.

[15] A. Spelde and C. Monahan, *Anesthesiology core review: Part 2, advanced exam. chapter 1: Invasive arterial blood pressure monitoring*, 2016.

[16] Y. Abuouf, S. Ookawara, and M. Ahmed, "Analysis of the effect of guidewire position on stenosis diagnosis using computational fluid dynamics," *Computers in Biology and Medicine*, vol. 121, p. 103 777, 2020.

[17] H. Kanai, M. Iizuka, and K. Sakamoto, "One of the problems in the measurement of blood pressure by catheter-insertion: Wave reflection at the tip of the catheter," *Medical and biological engineering*, vol. 8, no. 5, pp. 483–496, 1970.

[18] F. Stam, H. Kuisma, F. Gao, *et al.*, "Integration of a capacitive pressure sensing system into the outer catheter wall for coronary artery ffr measurements," in *Bio-MEMS and Medical Microdevices III*, International Society for Optics and Photonics, vol. 10247, 2017, p. 1 024 703.

[19] Radcliffe Cardiology, *Fractional flow reserve*, [Apr 2022], 2013. [Online]. Available: www.radcliffecardiology.com/articles%20fractional-flow-reserve-ffr-%20shown-%20improve-patient-outcomes-and-%20reduce-costs-0.

[20] M Elmasry, *Ffr threshold for ischemia*, [Apr 2022], 2014. [Online]. Available: www.slideshare.net/magdyelmasry1422/coronary-microvascular-%20dysfunction.

[21] J. Wang and K. Parker, "Wave propagation in a model of the arterial circulation," *Journal of biomechanics*, vol. 37, no. 4, pp. 457–470, 2004.

[22] S. P. Glasser, D. K. Arnett, G. E. McVeigh, *et al.*, "Vascular compliance and cardiovascular disease: A risk factor or a marker?" *American Journal of Hypertension*, vol. 10, no. 10, pp. 1175–1189, 1997.

[23] A. R. Pries, T. Secomb, T. Gessner, M. Sperandio, J. Gross, and P. Gaehtgens, "Resistance to blood flow in microvessels in vivo.," *Circulation research*, vol. 75, no. 5, pp. 904–915, 1994.

[24] Harvard Apparatus, *Pulsatile blood pump*, [Apr 2022], 2020. [Online]. Available: https://www.harvardapparatus.com/pumps-liquid-handling/pulsatile-blood-pumps.html.

[25] WW LaMorte, Phd, *Systolic and diastolic blood pressures*, [Apr 2022], 2016. [Online]. Available: ,%20www.sph-%20web.bumc.bu.edu/otlt%20mph-modules/ph/ph709%20heart/ph709%20heart10.html.

[26] T. Maruhashi, M. Kajikawa, S. Kishimoto, *et al.*, "Upstroke time is a useful vascular marker for detecting patients with coronary artery disease among subjects with normal ankle-brachial index," *Journal of the American Heart Association*, vol. 9, no. 23, e017139, 2020.

[27] G. Sainas, R. Milia, G. Palazzolo, *et al.*, "Mean blood pressure assessment during post-exercise: Result from two different methods of calculation," *Journal of Sports Science & Medicine*, vol. 15, no. 3, p. 424, 2016.

[28] A. J. Bank and D. R. Kaiser, "Smooth muscle relaxation: Effects on arterial compliance, distensibility, elastic modulus, and pulse wave velocity," *Hypertension*, vol. 32, no. 2, pp. 356–359, 1998.

[29] J.-H. Jeong, Y.-M. Kim, B. Lee, *et al.*, "Design and evaluation of enhanced mock circulatory platform simulating cardiovascular physiology for medical palpation training," *Applied Sciences*, vol. 10, no. 16, p. 5433, 2020.

[30] T. D. Homan, S. Bordes, and E. Cichowski, "Physiology, pulse pressure," 2018.

[31] UtahMedical Products, Inc, *Deltran blood pressure transducers*, [Apr 2022], 2022. [Online]. Available: http://www.utahmed.com/oem-pressure-transducers.html..

[32] IFM Efector, Inc, *Sm6004, magnetic-inductive flow meter*, [Apr 2022], 2022. [Online]. Available: www.ifm.com/us/en/product/SM6004.

[33] F. Otto, "Die grundform des arteriellen pulses," *Zeitung fur Biologie*, vol. 37, pp. 483–586, 1899.

[34] N. Westerhof, N. Stergiopulos, M. I. Noble, and B. E. Westerhof, *Snapshots of hemodynamics: an aid for clinical research and graduate education*. Springer, 2010, vol. 7.

[35] P. Boutouyrie, M. Briet, C. Collin, S. Vermeersch, and B. Pannier, "Assessment of pulse wave velocity," *Artery Research*, vol. 3, no. 1, pp. 3–8, 2009.

[36] N. Xiao, J. Alastruey, and C. Alberto Figueroa, "A systematic comparison between 1-d and 3-d hemodynamics in compliant arterial models," *International journal for numerical methods in biomedical engineering*, vol. 30, no. 2, pp. 204–231, 2014.

[37] SimVascular Development Team, *Coronary normal*, [Apr 2022], 2017. [Online]. Available: https://simvascular.github.io/clinicalCase3.html.

[38] E. Nader, S. Skinner, M. Romana, *et al.*, "Blood rheology: Key parameters, impact on blood flow, role in sickle cell disease and effects of exercise," *Frontiers in physiology*, p. 1329, 2019.

[39] K. Perktold, G. Karner, A. Leuprecht, and M. Hofer, "Influence of non-newtonian flow behavior on local hemodynamics," *ZAMM-Journal of Applied Mathematics and Mechanics/Zeitschrift Für Angewandte Mathematik Und Mechanik*, vol. 79, no. S1, pp. 187–190, 1999.

[40] D. McDonald and E. Attinger, "The characteristics of arterial pulse wave propagation in the dog," *Inf Exchange Group*, no. 3, 1965.

[41] R. Kampalath. "The Anatomy of the External Iliac Artery kernel description." (2020), [Online]. Available: https://www.verywellhealth.com/external-iliac-artery-anatomy-4692283.

.

A. BILL OF MATERIALS

This section will list the components described in the previous sections.

Table A.1. Bill of Materials – for full system components

Bill of Materials				
ITEM	Part Number	Description	Manufacturer	QTY.
Harvard Apparatus Pulsatile Blood Pump - 1423	MA1 55-3305	Pulsatile Blood Pump	Harvard Apparatus: Harvard Biosciences	1
Deltran Pressure Transducer	DPT-100	Deltran Disposable Pressure Transducer	Utah Medical Products Inc.	3
IFM Efector SM6004	SM6004	Magnetic Inductive Flow Meter	IFM Efector, Inc.	3
Versilon SPX-50 SAINT-GOBAIN Silicone Tubing	SPX-50	Silicone Tubing	Saint-Gobain	3 meter
Precision Flow-Adjustment ValveShutoff Valves	46425K14	Easy Set Adjustment Flow Valve	McMaster-Carr	3
VWR 200ml Compliance Chambers	VWR 75875-308	Tempered Glass Storage Chamber	VWR Intl.	3
3-D Pinted Vessel	N/A	Resin Printed 3-D Vessel Print	3-D Stereolithography Printer	1
Lab PC w/ LabVIEW Software	N/A	LabVIEW - Virtual Engineering Instrument Workpench	National Instruments	1
DAQ Hardware	NI-9203 NI-9201 NI-9174 cDAQ Amplifier Circuit	c Series Current Input Module c Series Voltage Input Module DAQ-Chassis	National Instruments	1 ea.